Technical Report

Reservoir Characterization Research Laboratory

Carbonate Reservoirs

Effects of Stratal Architecture and Diagenesis on Reservoir Development in the Grayburg Formation: South Cowden Field, Ector County, Texas

Stephen C. Ruppel and Don G. Bebout

Funding for this research was provided by Amoco, Aramco, ARCO, British Petroleum, Chevron, ELF, Exxon, Fina, JNOC, Marathon, Meridian, Oxy International, Oxy USA, PD Oman, Pennzoil, Phillips, Shell Canada, Shell Oil, Texaco, TOTAL, and Unocal.

Bureau of Economic Geology
Noel Tyler, Director
The University of Texas at Austin
Austin, Texas 78713-8924

October 1995

CONTENTS

Figures

Table

ABSTRACT

The Grayburg Formation in the South Cowden field of eastern Ector County displays an internal stratal architecture that typifies Grayburg shallow-water platform successions throughout the Permian Basin. Study of core and wireline logs in South Cowden field documents three orders of cyclicity in the Grayburg. The entire Grayburg constitutes a single long-duration accommodation cycle that commenced with a major sea-level rise and flooding of the preexisting San Andres platform and ended with a major basinward shift in facies associated with sea-level fall prior to deposition of Queen Formation tidal-flat successions. Four high-frequency sequences are recognized within the Grayburg that correspond to higher frequency sea-level rise events. The basal Grayburg sequence consists of backstepping, low-energy, mud-dominated cycles and is not a contributor to production in the field. Grayburg sequence 2 documents extensive flooding of the San Andres platform by outer ramp fusulinid wackestone-packstone facies and subsequent aggradation of an extensive tidal-flat-capped, grain-dominated packstone-grainstone ramp crest succession. Renewed platform transgression in Grayburg sequence 3, demonstrated by even more extensive onlap of the platform by fusulinid facies, documents a maximum flooding event that is correlatable throughout the Grayburg in both outcrop and subsurface. This event forms the basis for correlation of the Grayburg succession throughout the Permian Basin. Grayburg sequence 4 reflects highstand reduction of platform-to-basin relief and a major basinward shift in facies tracts.

High-frequency cyclicity is variably developed in the Grayburg, reflecting variations in platform accommodation and delivery of siliciclastics. In lower Grayburg transgressive sequences, cyclicity is poorly displayed because of lack of internal organization in outer ramp fusulinid-dominated succession and facies amalgamation in high-energy windward ramp crest successions. Highstand sequences, on the other hand, display well-developed, highly correlative, high-frequency cycles because of low platform relief and sufficient facies contrast between base

of cycle mud-dominated facies and cycle-capping peloid/ooid grain-dominated packstones and grainstones of the leeward back ramp crest.

Two major diagenetic events strongly affect reservoir character in some parts of the field. Recrystallized dolomite is developed along vertical burrows in highly cyclic mud-dominated packstones and wackestones of the HFS 4 Grayburg highstand succession. Later alteration and removal of anhydrite are focused in structurally low sections along the eastern and southern margins of the field. Where the products of these two events overlap, original depositional heterogeneities are muted.

Multiple hierarchies of cyclicity documented for the Grayburg constitute a sophisticated high-resolution reservoir architectural framework. Although the components of this framework vary, the fundamental style can provide a basis for characterizing many Grayburg shallow platform reservoirs in the Permian Basin.

Recognizing the controls and distribution of the diagenetic overprint of original architectural elements, however, is crucial to developing an accurate model of each Grayburg reservoir succession.

INTRODUCTION

As a group, middle Permian restricted, shallow-water carbonate platform reservoirs in the Permian Basin contain the largest hydrocarbon resource in the state of Texas (Galloway and others, 1983; Tyler and others, 1984; Tyler and Banta, 1989). Ruppel and others (1995) calculated that these reservoirs, which are developed in the San Andres and Grayburg Formations (Leonardian–Guadalupian) and in the Clear Fork Group (Leonardian), have already accounted for more than 12.5 billion barrels of oil (fig. 1). Because of low recovery efficiencies, as much as 17 billion barrels of mobile oil still remain in these rocks.

Recovery of the large remaining resource in Permian shallow-water carbonate platform reservoirs depends on a better understanding of the geologically controlled heterogeneity that controls production. To confront this issue, the Bureau of Economic Geology began detailed

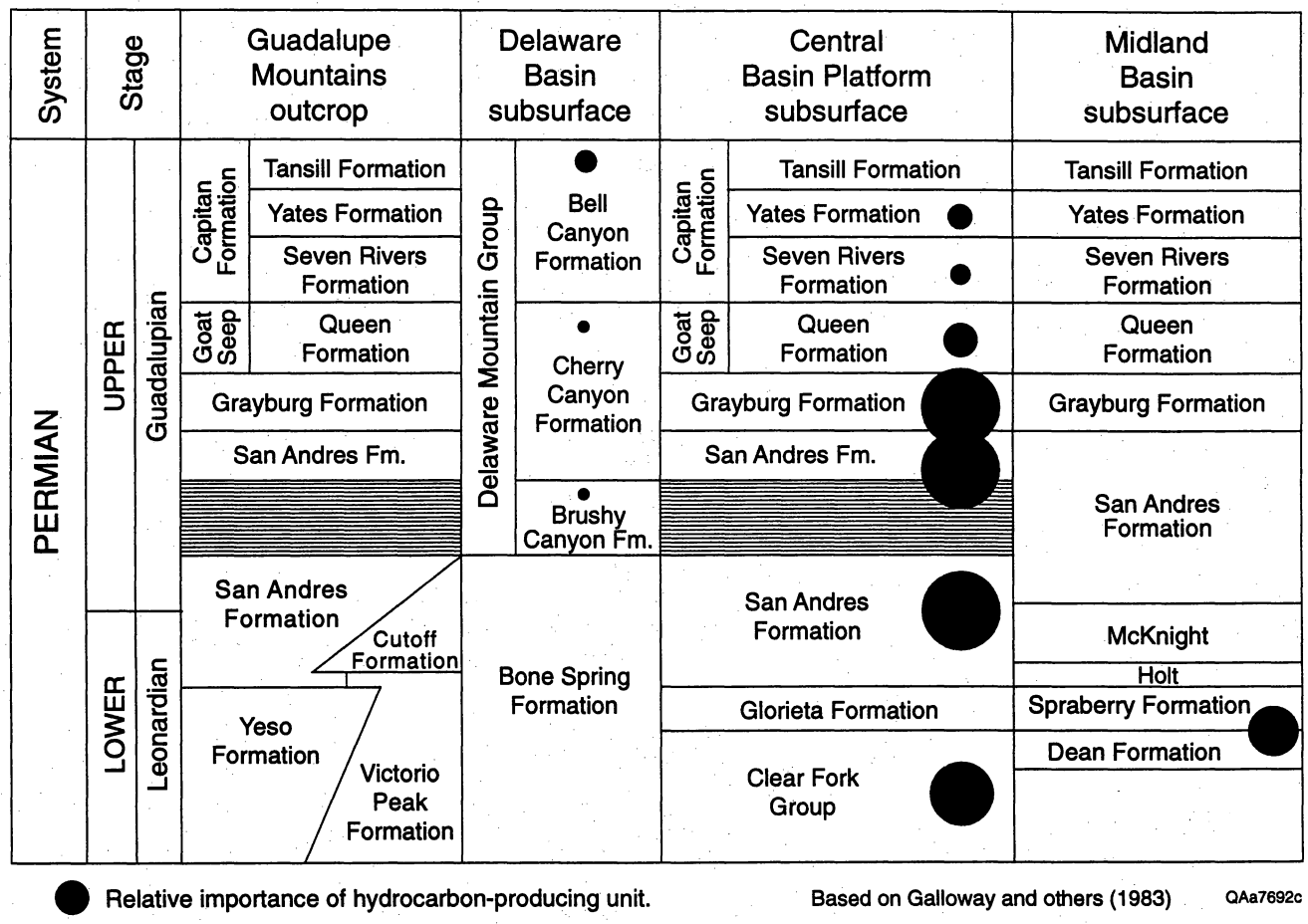

Figure 1. General correlations and stratigraphic nomenclature of upper Leonardian and Guadalupian (middle Permian) strata in the Permian Basin, West Texas and New Mexico. Note that most hydrocarbon production has come from Clear Fork, San Andres, and Grayburg reservoirs.

studies of these reservoirs more than 10 years ago. In recent years, geological aspects of this research have included (1) development of outcrop-based reservoir analog models using a sequence stratigraphic approach (for example, Kerans and others, 1994), (2) regional subsurface studies designed to form a framework for applying outcrop models to reservoirs, and (3) detailed characterization of reservoir framework. In each of these research areas, a sequence stratigraphic or cycle stratigraphic approach has been used to improve characterization and to facilitate integration and synthesis.

These studies have concentrated primarily on reservoirs and equivalent outcrops in the San Andres and Grayburg Formations. Fundamental geological models of San Andres reservoirs were developed in outcrop (Kerans and others, 1994) and were applied to the producing subsurface fields (Lucia and others, 1995). Similar outcrop studies were undertaken for the Grayburg Formation (Kerans and Nance, 1991) and are ongoing (Barnaby and Ward, 1994, 1995). Our report presents the results of geological characterization studies in a typical Grayburg reservoir in the Permian Basin. The purpose of this work is to apply geological models developed in outcrop studies to better constrain the geological reservoir framework and heterogeneity in a typical Grayburg reservoir, the South Cowden Grayburg reservoir. This framework provides a strong basis for defining petrophysical and flow unit properties in the reservoir and serves as a prototype model for other Grayburg reservoir characterization studies.

SETTING

The South Cowden Grayburg reservoir is located on the eastern margin of the Central Basin Platform in eastern Ector County, immediately southwest of Odessa, Texas (fig. 2). Like most San Andres and Grayburg reservoirs, South Cowden is situated on the outer part of the shallow-water Grayburg platform. Oil was first discovered in the South Cowden field area (then called the Addis field) in 1933 (Young and Vaughn, 1957). The field now occupies part of an essentially continuous trend of productive Grayburg extending north into the Foster and Johnson fields.

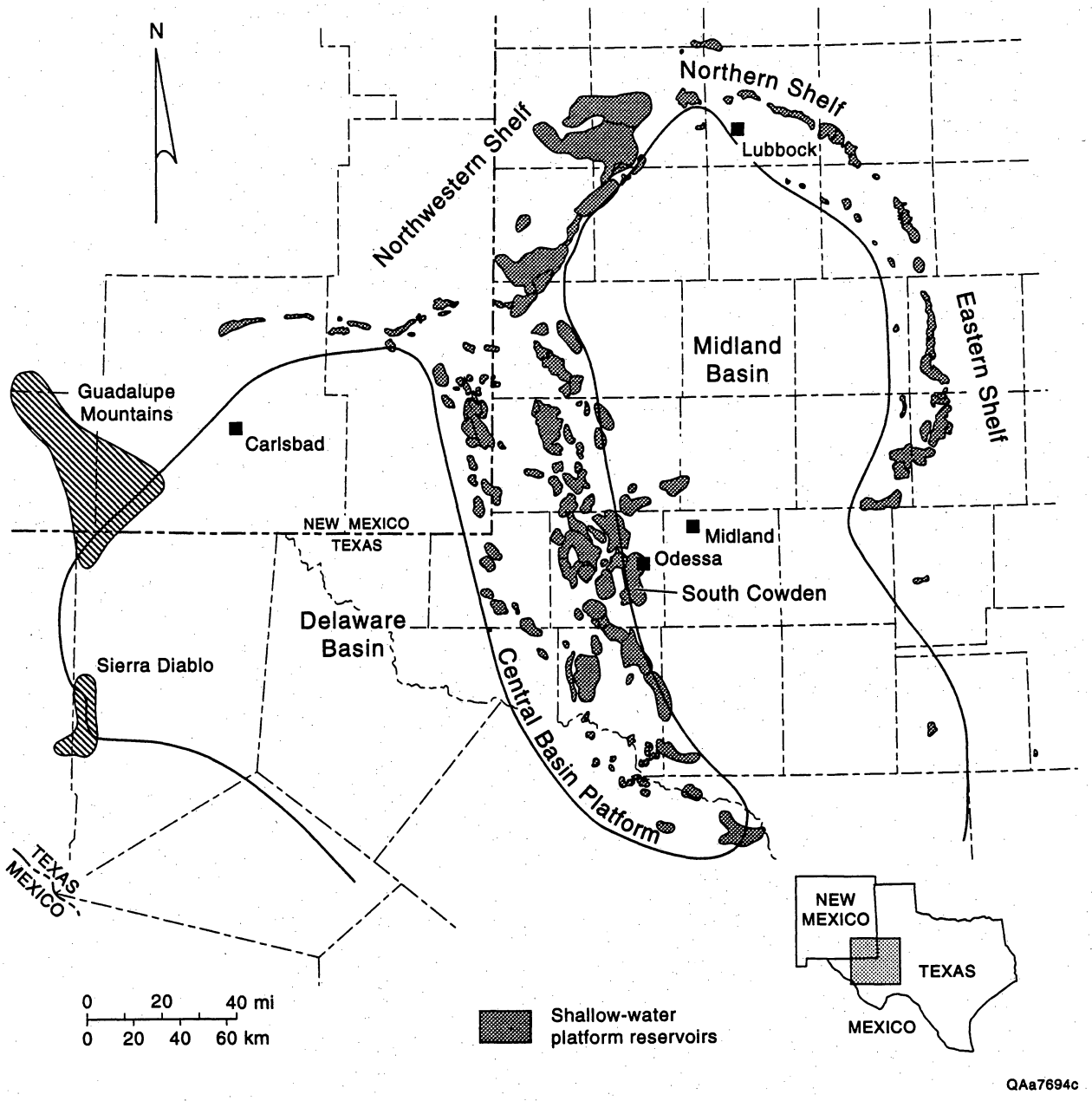

Figure 2. Map showing the Guadalupian paleogeography of West Texas and New Mexico and the distribution of major shallow-water platform carbonate reservoirs, including those productive from the Grayburg Formation.

South Cowden field is subdivided into several productive units. Most production, however, has come from the Fina Emmons Unit, the Phillips South Cowden Unit, and the UNOCAL Moss Unit (fig. 3). We confined our study largely to these areas, where sufficient data were available. Total oil production from the Grayburg in South Cowden field totaled 154 million barrels as of January 1, 1994; the Emmons, South Cowden, and Moss Units have been the most highly productive parts of the field. All units are currently under waterflood.

Regional structure-contour mapping of the Grayburg Formation illustrates that the study area in South Cowden field occupies a structural salient into the Midland Basin. This feature trends southeastward from the predominantly northeast-striking platform at a 90-degree angle.

METHODS

Wireline logs were obtained for approximately 400 wells in the South Cowden field area. Cores and core analysis data were obtained for 27 wells (fig. 3). Nearly 6,000 ft of core was described on an inch-by-inch basis using a cycle stratigraphic approach. Thin sections were prepared for confirmation of facies identifications and definition of diagenetic relationships. Core-defined cycles were calibrated to wireline logs and correlated across the field. Isopach and structure maps were prepared for each cycle and cycle set. The resulting data were used to create a three-dimensional (3-D) reservoir framework model using Strata Model Geocellular Modeling software.*

UNOCAL and Phillips provided 3-D seismic data for much of the field. These data were used primarily to constrain sub-Grayburg reservoir horizons.

REGIONAL GEOLOGICAL SETTING

Synthesis of seismic data and deep wireline log data in the eastern Ector County area helped to elucidate the pre-Grayburg depositional history of the area. These data define the contact

*The use of firm and brand names in this report is for identification purposes only and does not constitute endorsement by the Bureau of Economic Geology.

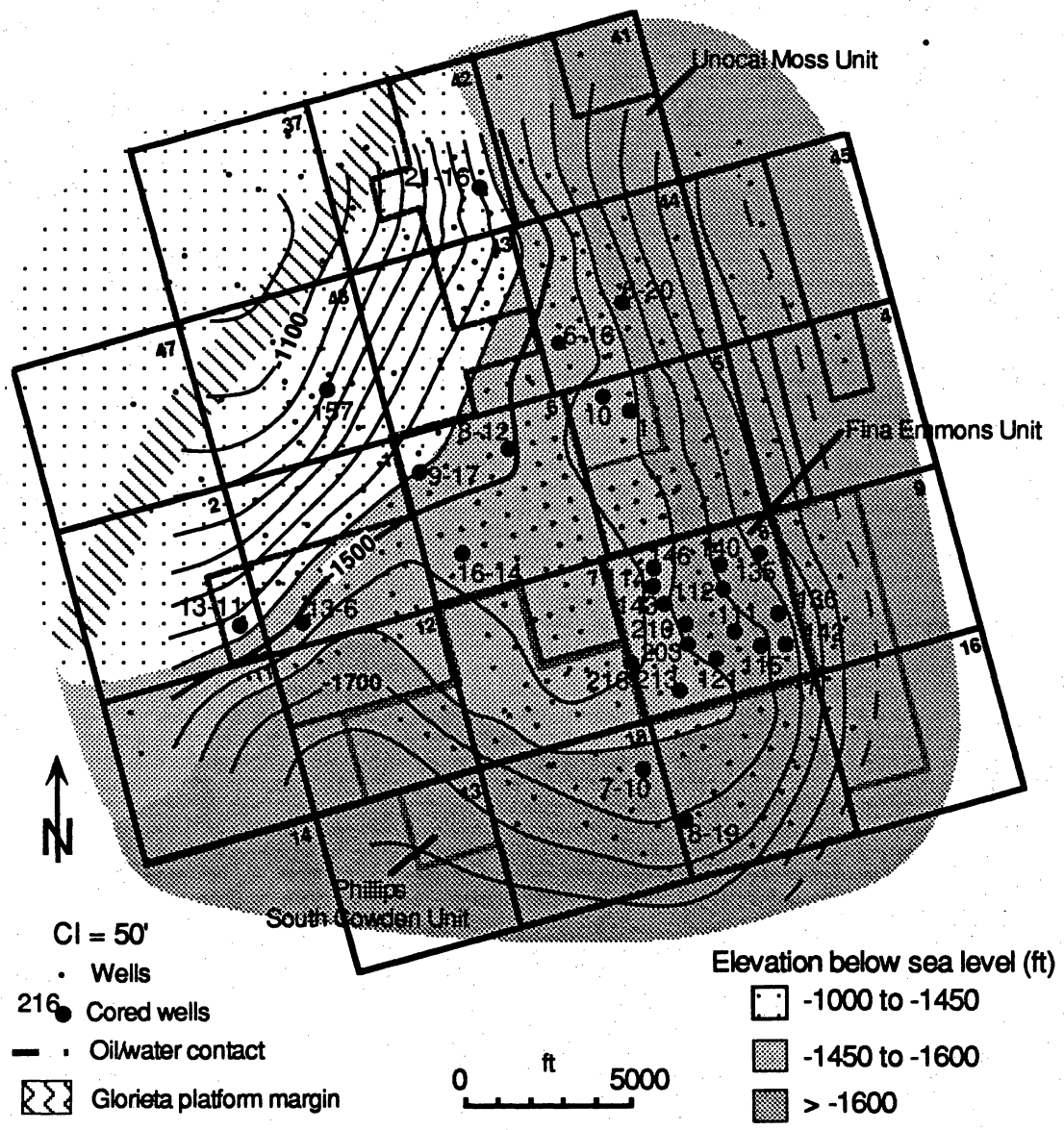

Figure 3. Map of South Cowden field showing the structure on top of the Grayburg Formation and the area of study. Locations of cored wells and major cross sections referenced in this report shown.

between the Glorieta Formation and the overlying San Andres very clearly in this area. This contact is a major third-order sequence boundary that separates late highstand, siliciclastic-bearing tidal-flat deposits of the Glorieta from transgressive, subtidal deposits of the basal San Andres (Ruppel, 1992; Kerans and others, 1994; Kerans and Ruppel, 1994). Seismic and log data demonstrate that the Glorieta platform margin dips at about 2.5 degrees eastward and trends generally north/northeastward through the South Cowden area (figs. 4 and 5).

The terminal Glorieta platform margin acted as a structural control for depositional patterns in the overlying Permian. Regional data indicate that many of the reservoirs productive from the Grayburg are situated on the outer margin of the Glorieta platform. Much of South Cowden field, however, is located east of the Glorieta margin on a southeast-trending structural salient that lies basinward of the margin (fig. 4). Seismic data suggest that this salient owes its origin to an underlying large depositional wedge. On 3-D seismic data, this wedge is characterized by progradational internal geometries with southeast-dipping clinoforms (fig. 6). Wireline-log and 2-D data indicate that the wedge is developed as a lobe-shaped feature that extends east/southeastward from the Glorieta margin. The axis of the wedge, defined by both clinoformal geometries and thickness patterns, trends southeastward immediately under the area of productive Grayburg wells in the South Cowden field. The effect of this depositional event is illustrated by time-structure maps depicting Glorieta and Grayburg paleotopography (figs. 7 and 8). Note that prior to the deposition of this progradational wedge, the structural grain was dominated by the northeast-trending Glorieta margin (fig. 7). Deposition of the southeast-trending progradational wedge (fig. 8) created a much different structural configuration, which affected depositional and thickness patterns throughout much of the rest of the Permian.

Both seismic and wireline-log data demonstrate that the progradational wedge stratigraphically overlies the Glorieta and is largely restricted to a position distal to the Glorieta platform margin. These relationships, combined with the internal geometry of the feature, suggest that it formed during a major sea-level fall as a lowstand progradational deposit. Interpretation of wireline logs and sample cuttings indicates that these deposits consist of

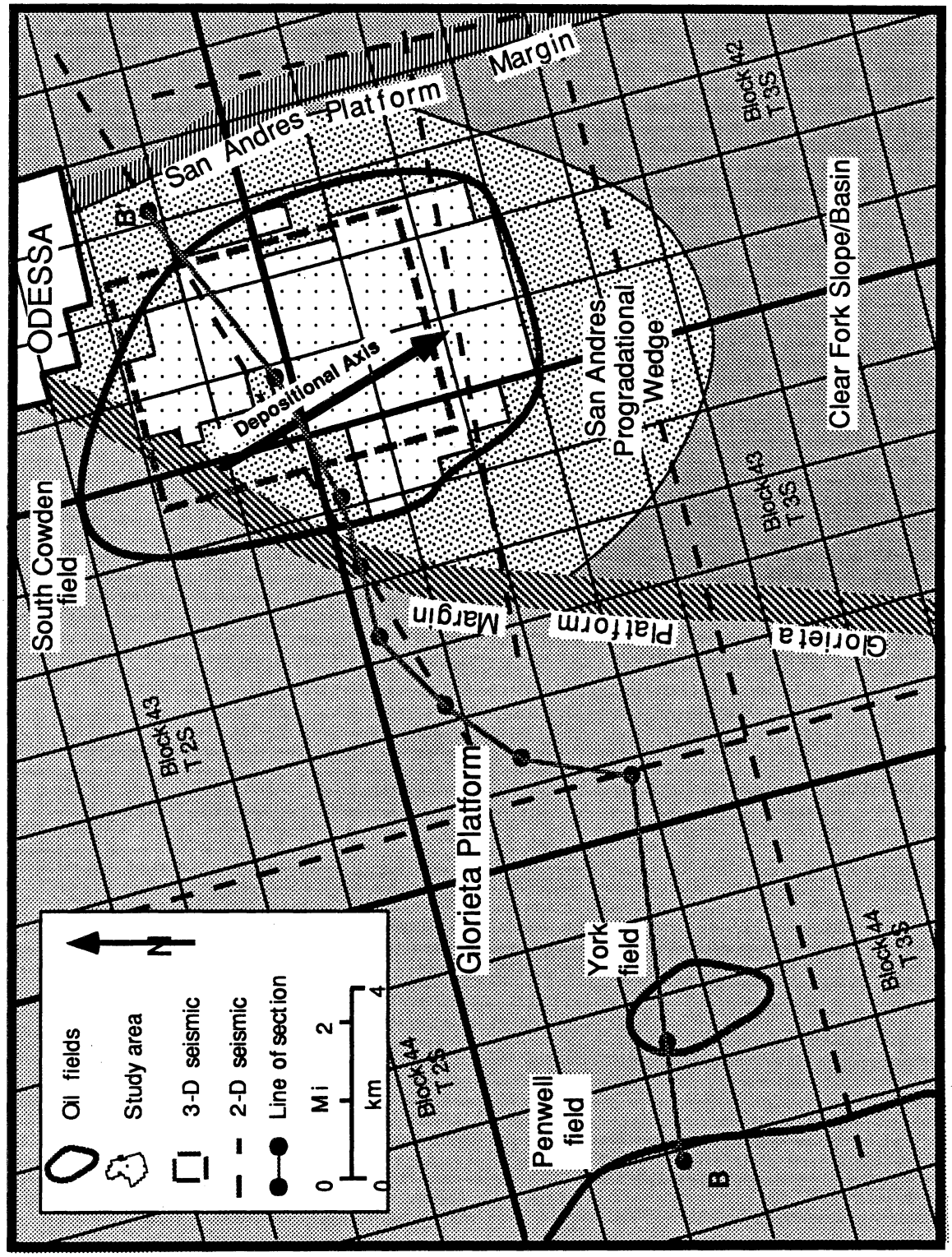

Figure 4. Map of eastern Ector County showing the distribution of major structural and depositional features in late Leonardian to Guadalupian time.

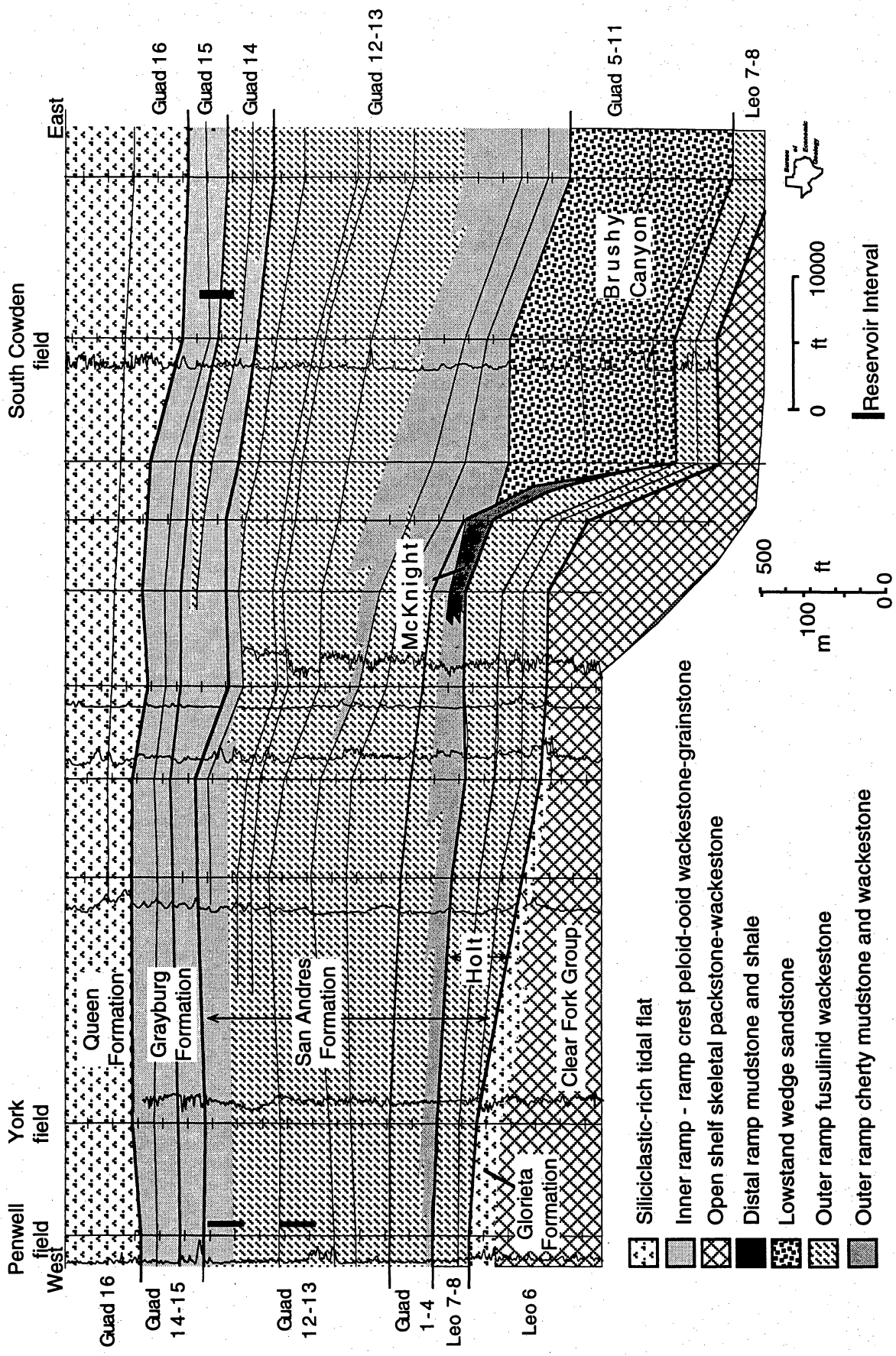

Figure 5. West-east wireline log cross section (A–A′) of Penwell field to South Cowden field showing general facies patterns, interfield correlations, and the position of the lower Guadalupian progradational wedge (probable Brushy Canyon equivalent) below the South Cowden field. Line of section is shown in figure 3.

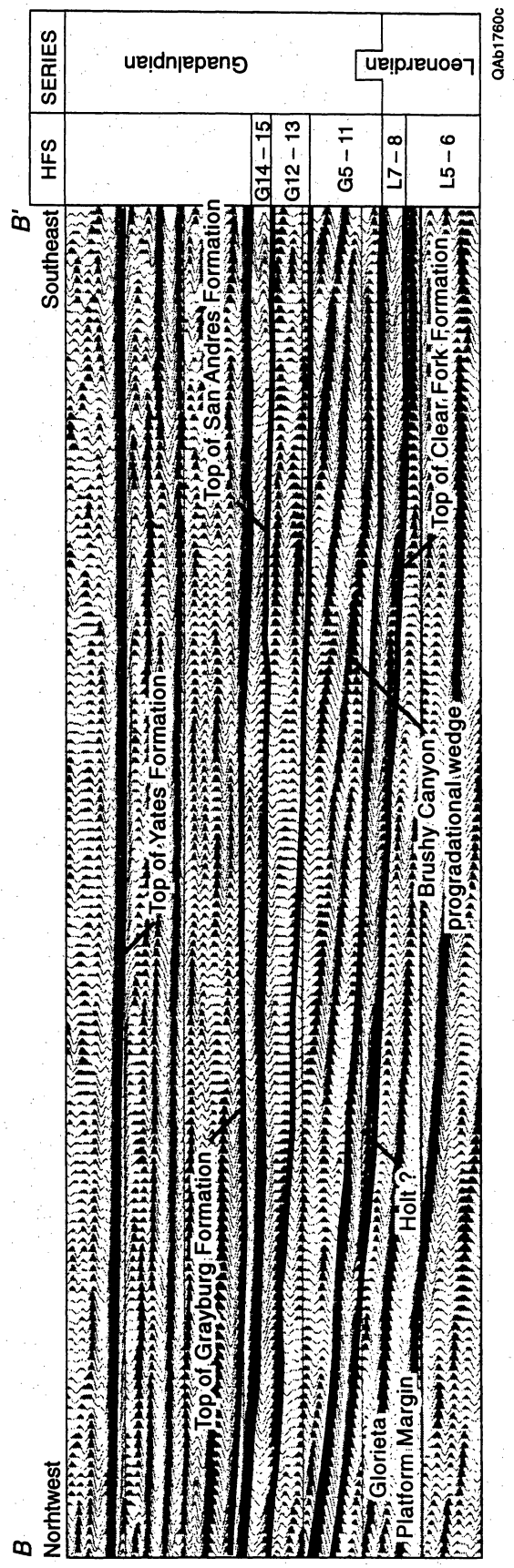

Figure 6. Southwest-trending three-dimensional seismic cross section (B–B′) through South Cowden field showing terminal Glorieta platform margin and overlying progradational wedge. Line of section shown in fig. 3.

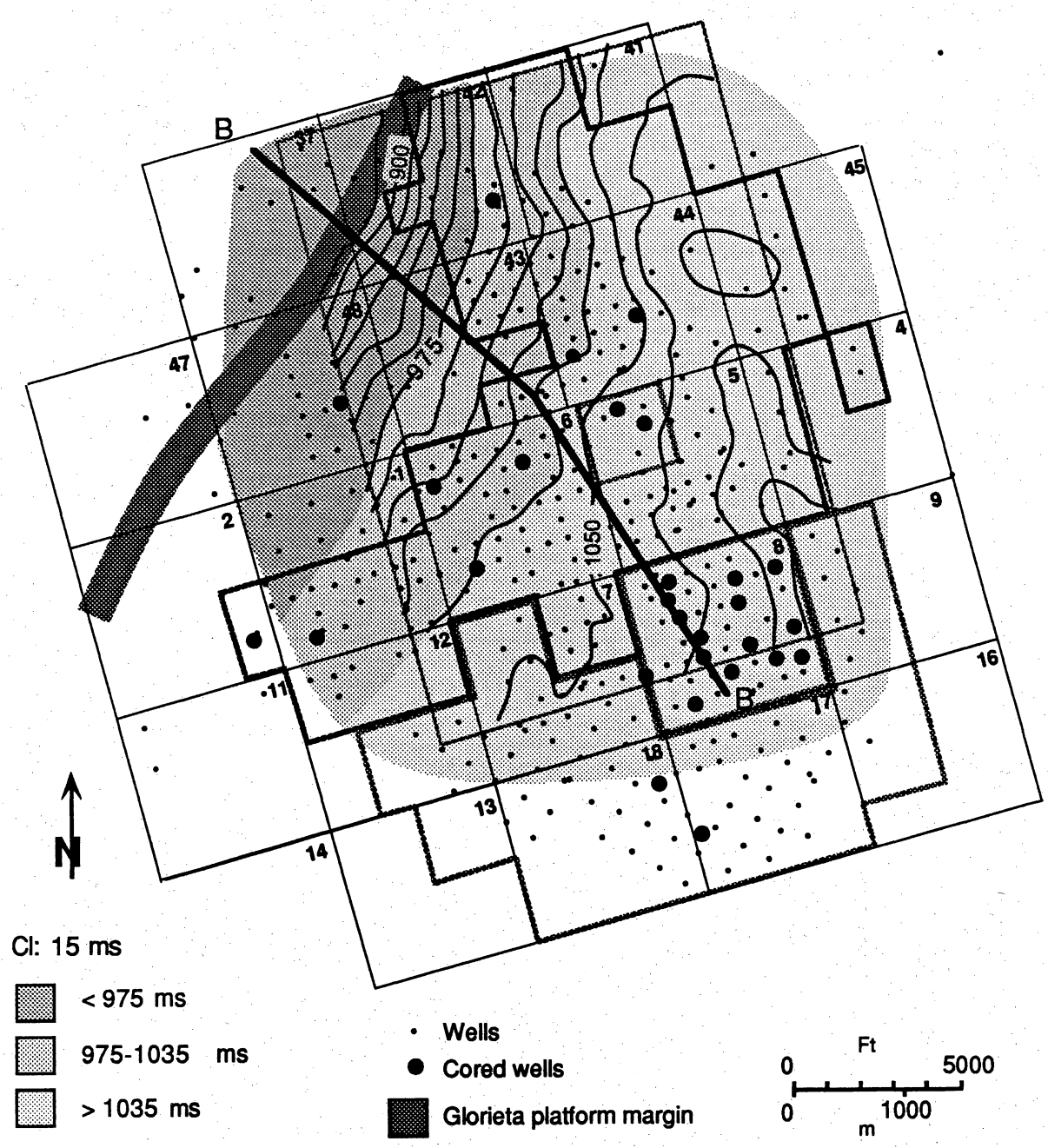

Figure 7. Seismic time-structure map showing the topography of the top of the Glorieta platform.

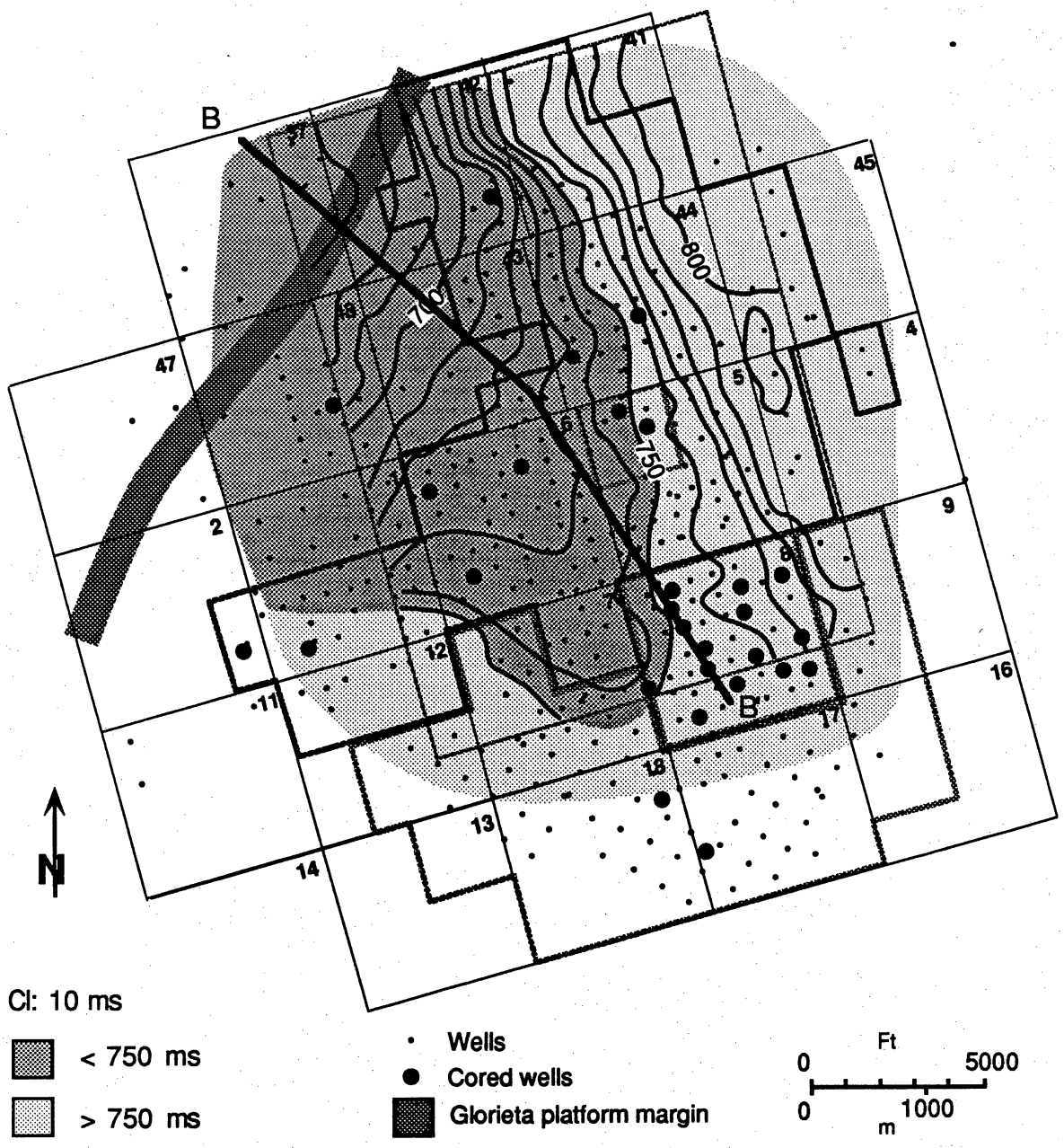

Figure 8. Seismic time-structure map showing the topography of the top of the Grayburg Formation in the South Cowden field.

substantial amounts of sandstone interbedded with dolostone. Such clastic-rich deposits are similar to sandstone/carbonate successions of the Spraberry Formation, which have been interpreted to represent episodic influx of resedimented carbonates, derived from the platform margin, and terrigenous clastics (Handford, 1981).

The precise stratigraphic and chronostratigraphic position of the post-Glorieta lowstand wedge is not definable from subsurface data. Almost certainly, it is related to either (1) the late Leonardian fall in sea level that immediately postdated terminal Glorieta deposition or (2) the early Guadalupian sea-level fall that followed lower San Andres deposition (Kerans and others, 1994; Kerans and Ruppel, 1994). A comparison with the well studied and the stratigraphically constrained equivalent section in the Guadalupe Mountains of West Texas suggests the latter is more likely.

The upper Leonardian Glorieta platform margin is well exposed along the Western Escarpment of the Guadalupe Mountains (fig. 9). Although much of the succession has not been studied in detail, basic stratigraphic relations of the major sequences are well established (Kerans and Fitchen, 1995). Upper Clear Fork and Glorieta subsurface intervals are represented on Cutoff Ridge and the Western Escarpment (fig. 10) by shallow-water platform carbonates and tidal flats, respectively, of the lower part of the Victorio Peak. Open marine, deeper water carbonates of the upper Victorio Peak Formation, which document a major transgression following post-Glorieta sea-level fall, are equivalent to basal San Andres strata, locally known as the Holt, in the subsurface (fig. 11). In the Guadalupe Mountains, the Cutoff Formation, a condensed section composed of lime mudstone (Harris, 1988) that is equivalent to much of the lower San Andres on the platform (Kerans and others, 1994), overlies the upper Victorio Peak. In the subsurface, the equivalent McKnight facies overlies the Holt along the eastern margin of the Central Basin Platform (fig. 11), where locally the Holt is productive and the McKnight serves as a top seal and possible source rock. Along the Western Escarpment, channeled Brushy Canyon sandstones overlie the Cutoff or, where the latter has been removed by erosion, the Victorio Peak (fig. 9) (Rossen and Sarg, 1988).

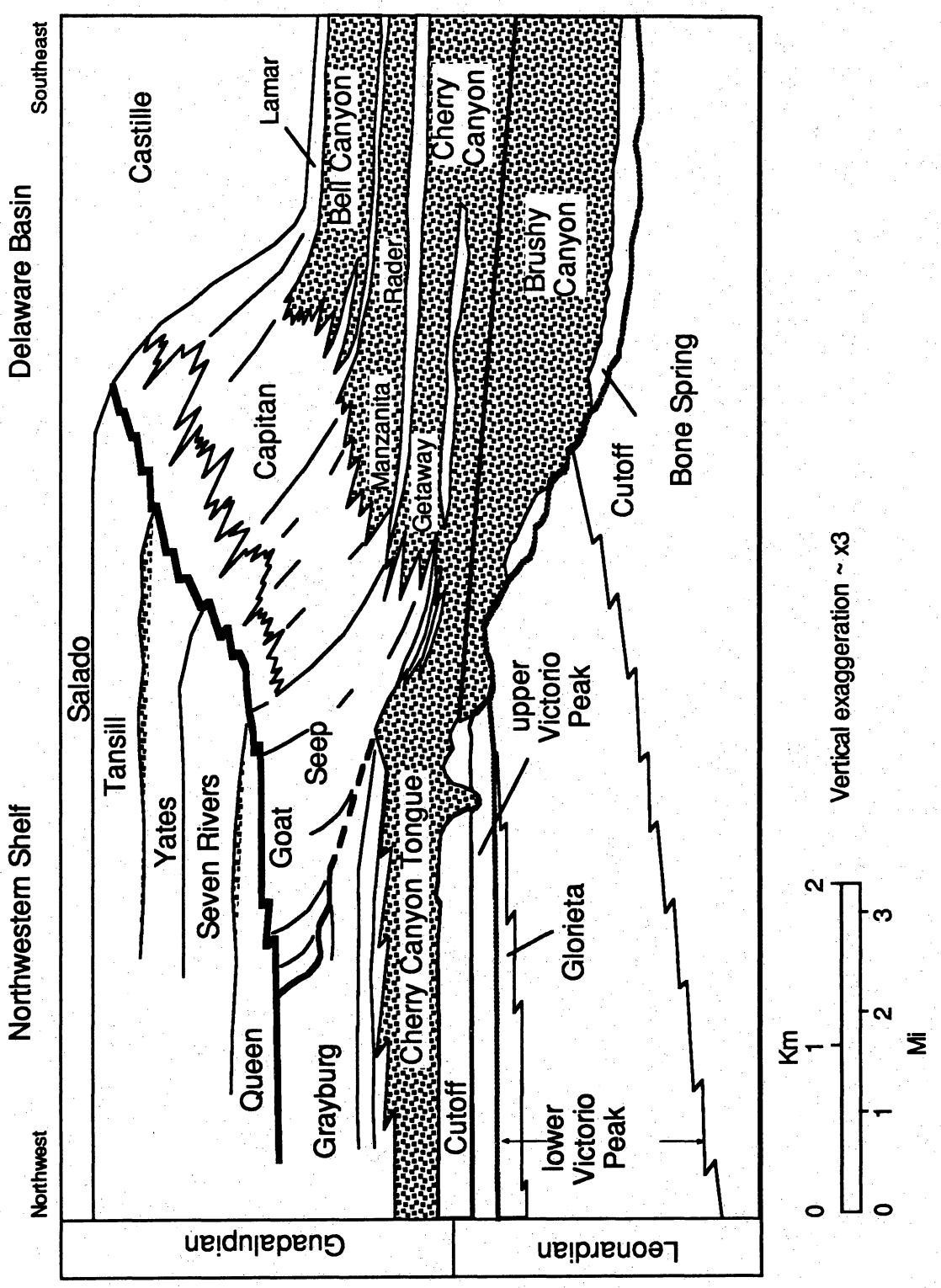

Figure 9. General stratigraphic relationships in the upper Leonardian–lower Guadalupian section on the Western Escarpment of the Guadalupe Mountains. From Pray (1988).

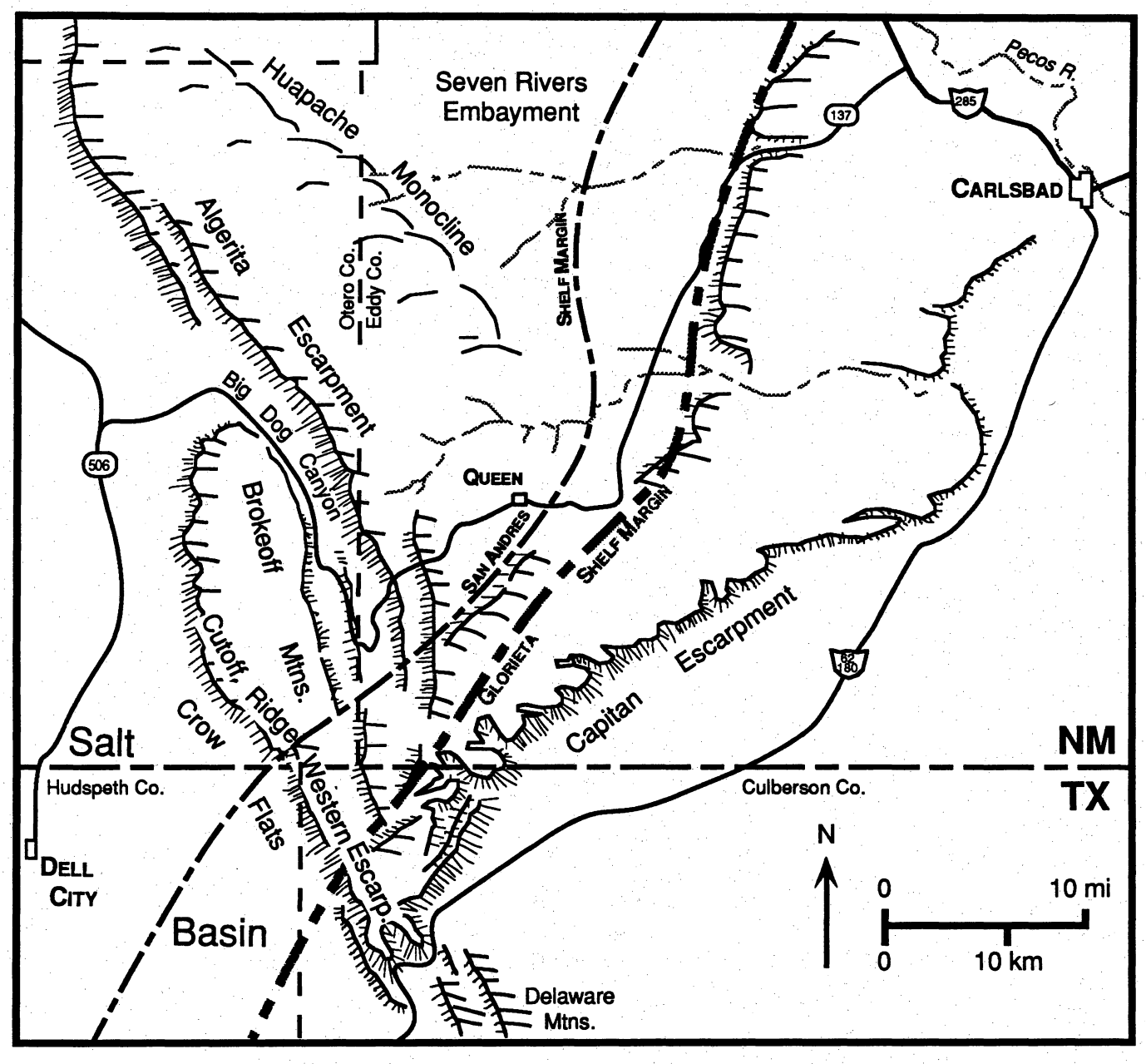

Figure 10. Map of the Guadalupe Mountains, Texas and New Mexico, showing location of major upper Leonard and lower Guadalupian outcrop localities. Modified from King (1948) and Babcock (1977).

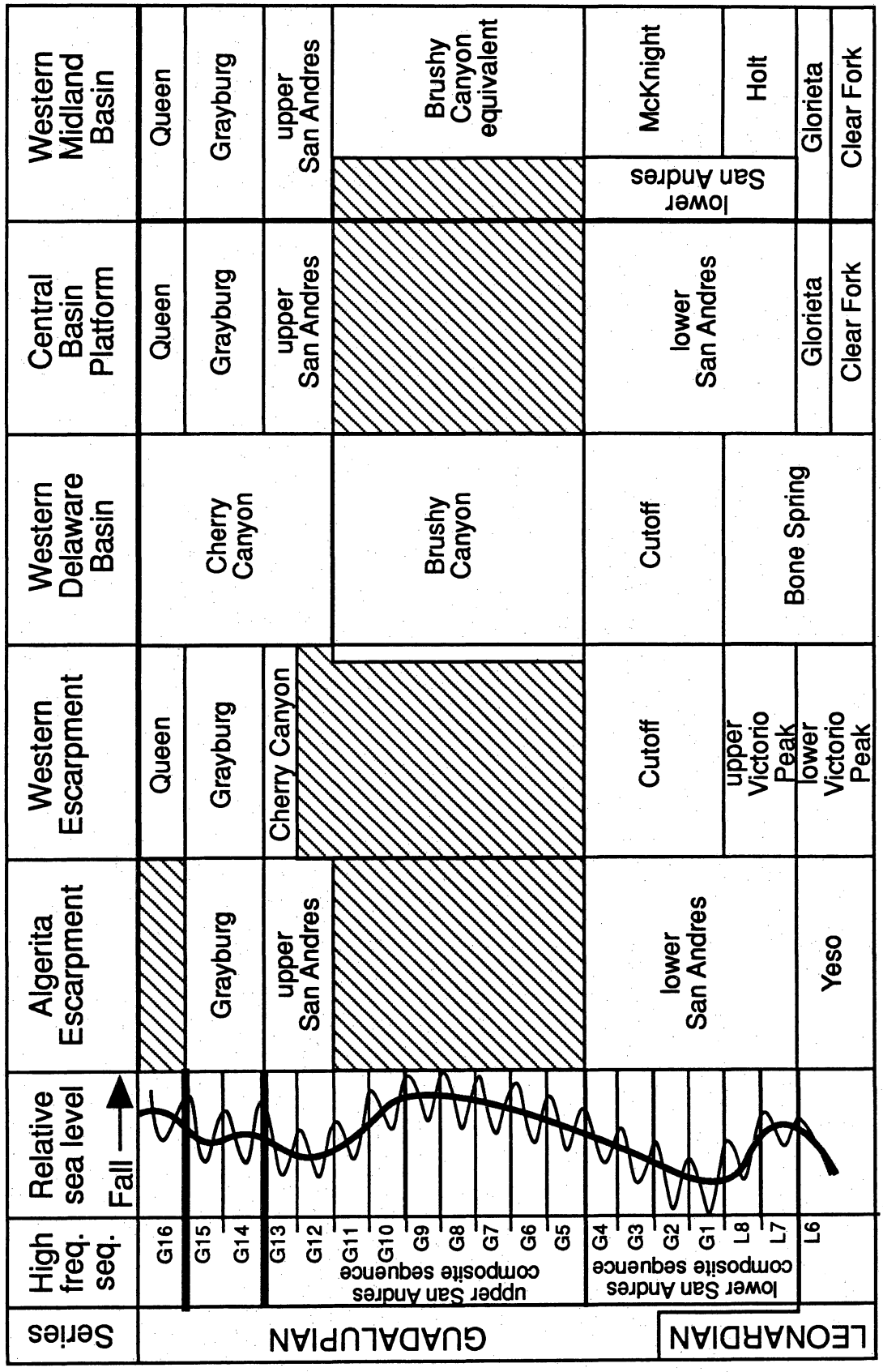

Figure 11. Sequence stratigraphy of the upper Leonardian and lower Guadalupian section in the Permian Basin. Modified from Kerans and Ruppel (1994).

Comparison of outcrop and subsurface cross sections reveals a close similarity in stratal relationships between the two areas, suggesting that the outcrop is an accurate analog for the subsurface. Although the subsurface McKnight appears to differ from its outcrop equivalent Cutoff in thickness and distribution, this difference may be caused by the scarcity of wireline and core data. The similarity between outcrop and subsurface sections implies that the progradational, clastic-dominated wedge in the eastern Ector County area is a direct equivalent of the Brushy Canyon sandstone and represents a lowstand wedge that accumulated during a major sea-level fall during middle San Andres (Guadalupian HFS 5 through HFS 11) time (fig. 12). If, however, equivalents of the Holt and McKnight overlie the progradational wedge, the latter represents an upper Leonardian, post-Glorieta, pre-San Andres lowstand wedge that has not previously been documented.

Whatever the age of the post-Glorieta progradational wedge in the South Cowden area, it is clear that it has served as a structural control for subsequent deposition in the area. The structural high that forms the South Cowden reservoir is virtually identical in shape and extent to this older feature. Preliminary examination of structural trends in other Grayburg fields along the eastern margin of the Central Basin Platform suggests that other reservoirs may owe their formation to similar underlying basin-restricted wedges.

GRAYBURG DEPOSITIONAL FACIES IN SOUTH COWDEN FIELD

The Grayburg Formation in South Cowden field contains six major depositional facies: (1) fusulinid wackestone-packstone, (2) peloid/ooid, grain-dominated packstone-grainstone, (3) peloid wackestone-packstone, (4) skeletal wackestone-packstone, (5) tidal-flat facies, and (6) sandstone-siltstone. As is typical of most Grayburg successions in the Permian Basin, all rocks have been dolomitized. These facies are virtually identical to those reported in other studies of both Grayburg and San Andres reservoir successions (Bebout and others, 1987; Major and others, 1988; Ruppel and Cander, 1988b; Tyler and others, 1992). Such assemblages typify shallow-water platform facies types for the entire middle Permian in the Permian Basin of West

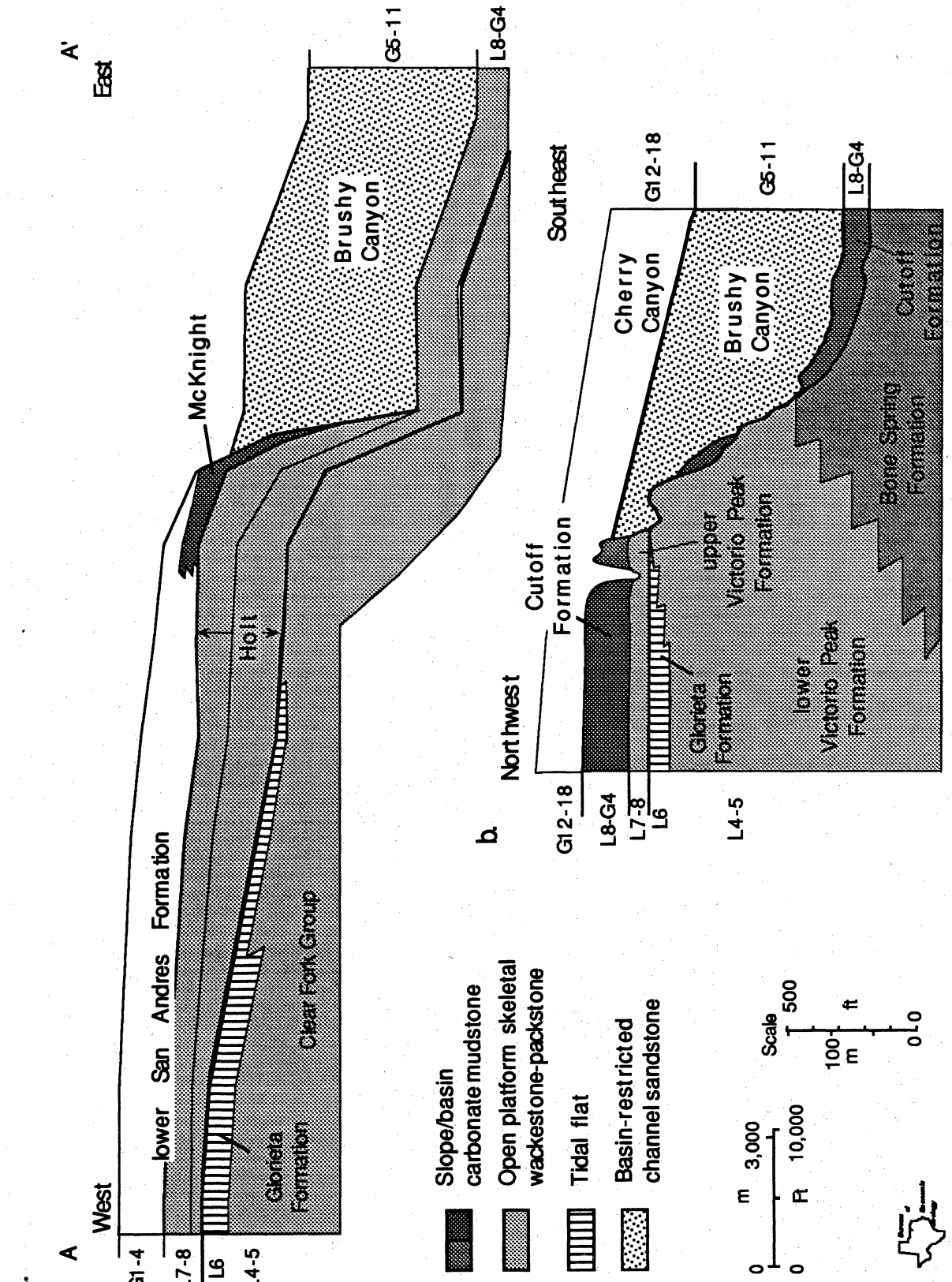

Figure 12. Comparison of the upper Leonardian to lower Guadalupian section in the South Cowden field (a) with the Western Escarpment of the Guadalupe Mountains (b). Outcrop section rescaled from Pray (1988) to match scale of subsurface section.

Texas and New Mexico (Ruppel and others, 1995). Figure 13 depicts the general distribution of these facies along an idealized inner platform to basin transect representative of the middle Permian.

General lateral facies relations across the South Cowden field area are illustrated in figure 14, which shows that the Grayburg was deposited during a long-term accommodation cycle on a west- to east-dipping ramp (fig. 14). More detailed study of lateral and vertical facies stacking patterns reveal that at least four higher frequency accommodation cycles, called high-frequency depositional sequences (HFS) after Kerans and others (1994), can be recognized within this long-duration cycle. Recognition of these facies and their depositional significance is fundamental to assembling a high-resolution, cycle stratigraphic framework of the reservoir succession. Figure 14 details the distribution of the four most significant of these facies along a platformward to basinward dip section.

Fusulinid Wackestone and Packstone

Fusulinid wackestones are most abundant in the eastern, downdip part of the field and in HFS 1, HFS 2, and HFS 3 (fig. 15a). These rocks typically contain 10 to 40 percent fusulinids and variable amounts of peloids; other skeletal debris, including pelmatozoans; and quartz silt-sand. In some successions, variations in the abundance of fusulinids and peloids define cycles of two types. Cycles defined by upward increases in abundance of fusulinids are most common in the eastern part of the field and in the lower parts of longer term cycles (that is, higher accommodation settings). Cycles composed of basal fusulinid wackestone and capping peloid-dominated packstones are more common in lower accommodation settings near the tops of longer term cycles. Neither "cycle" type is readily correlative among cored wells, perhaps because of their wide spacing, and neither generally possesses a recognizable log signature. Accordingly, these "cycles" are generally not correlatable.

Fusulinid facies typically contain common anhydrite in the form of nodules, void fillings, or poikilotopic masses. Porosity and permeability in these rocks is variable, depending on the

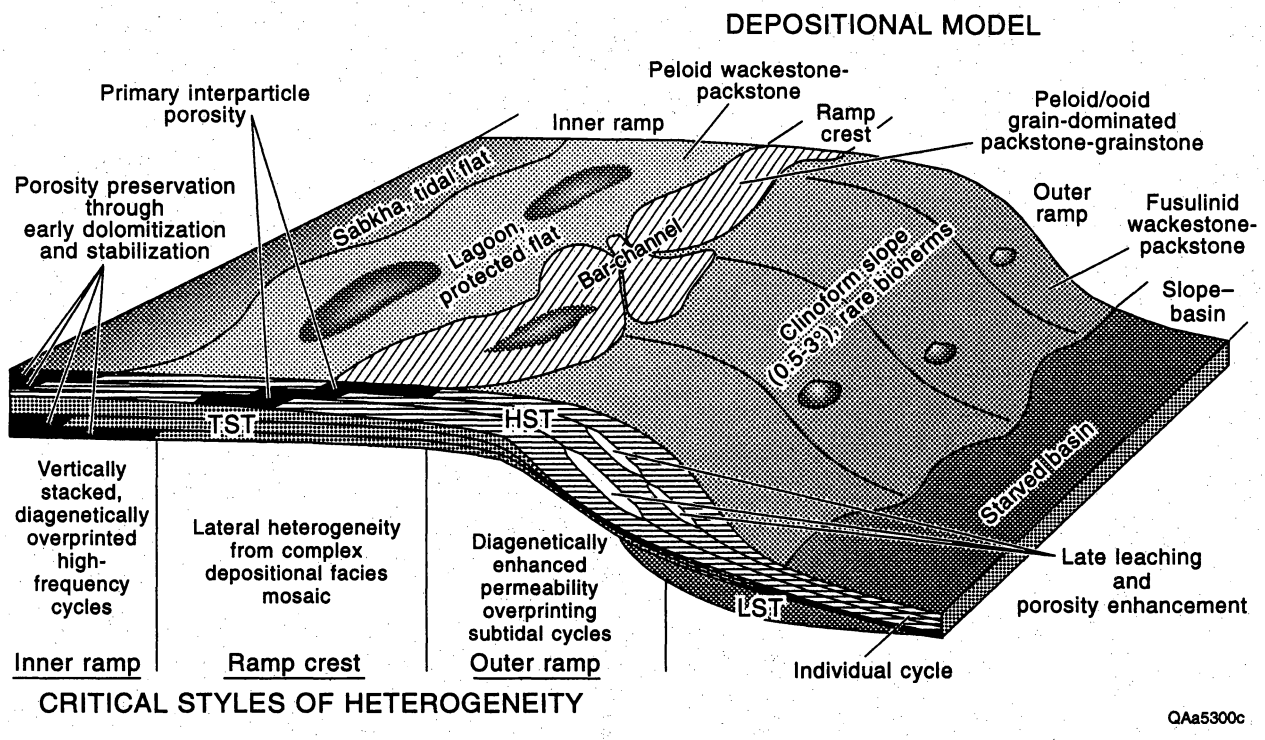

Figure 13. Generalized depositional model for middle Permian shallow-water carbonate platform succession in the Permian Basin. LST-lowstand systems tract, TST-transgressive systems tract, and HST-highstand systems tract. From Ruppel and others (1995).

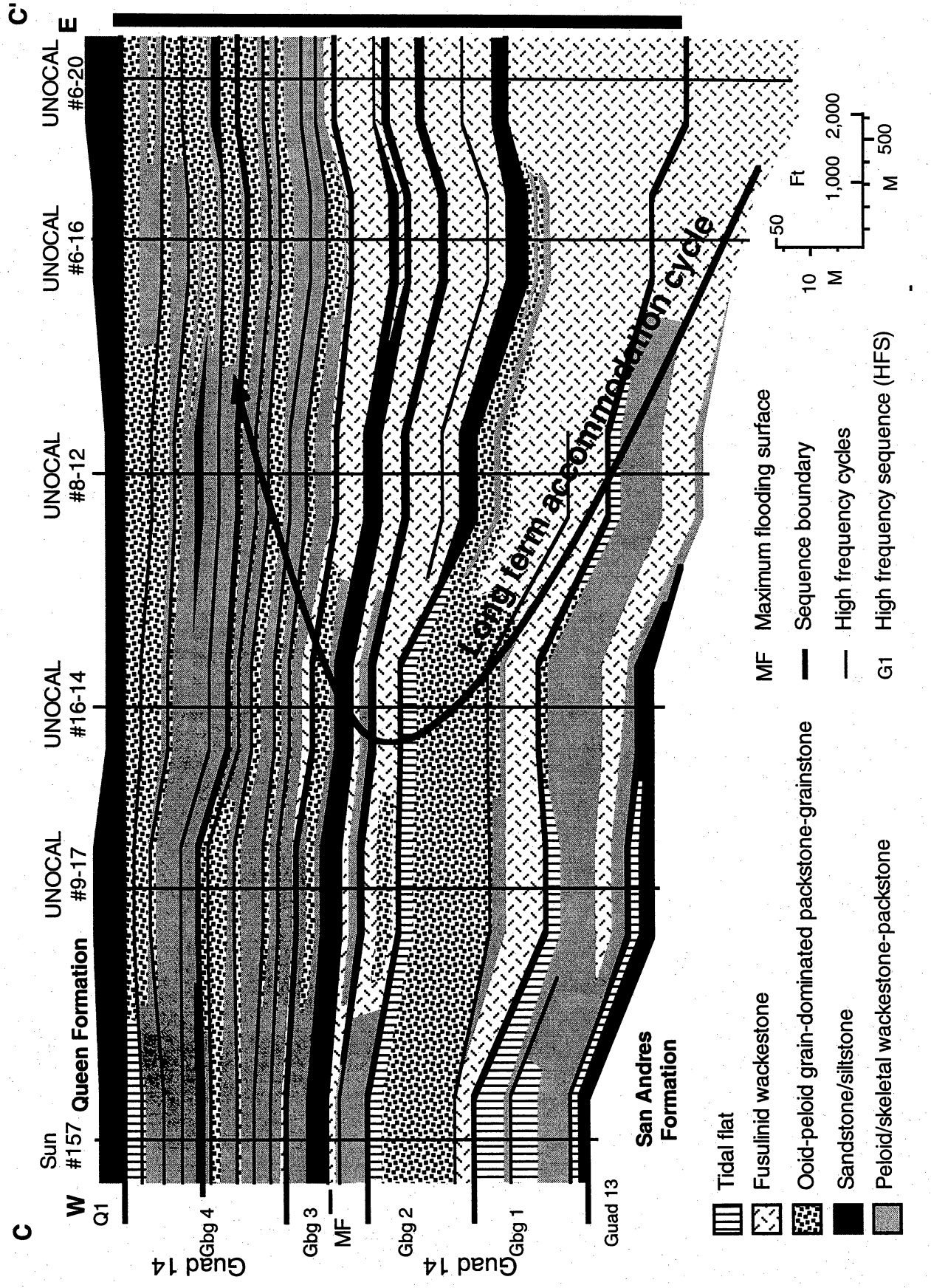

Figure 14. Grayburg sequence stratigraphic framework in the South Cowden field. Section approximates depositional dip.

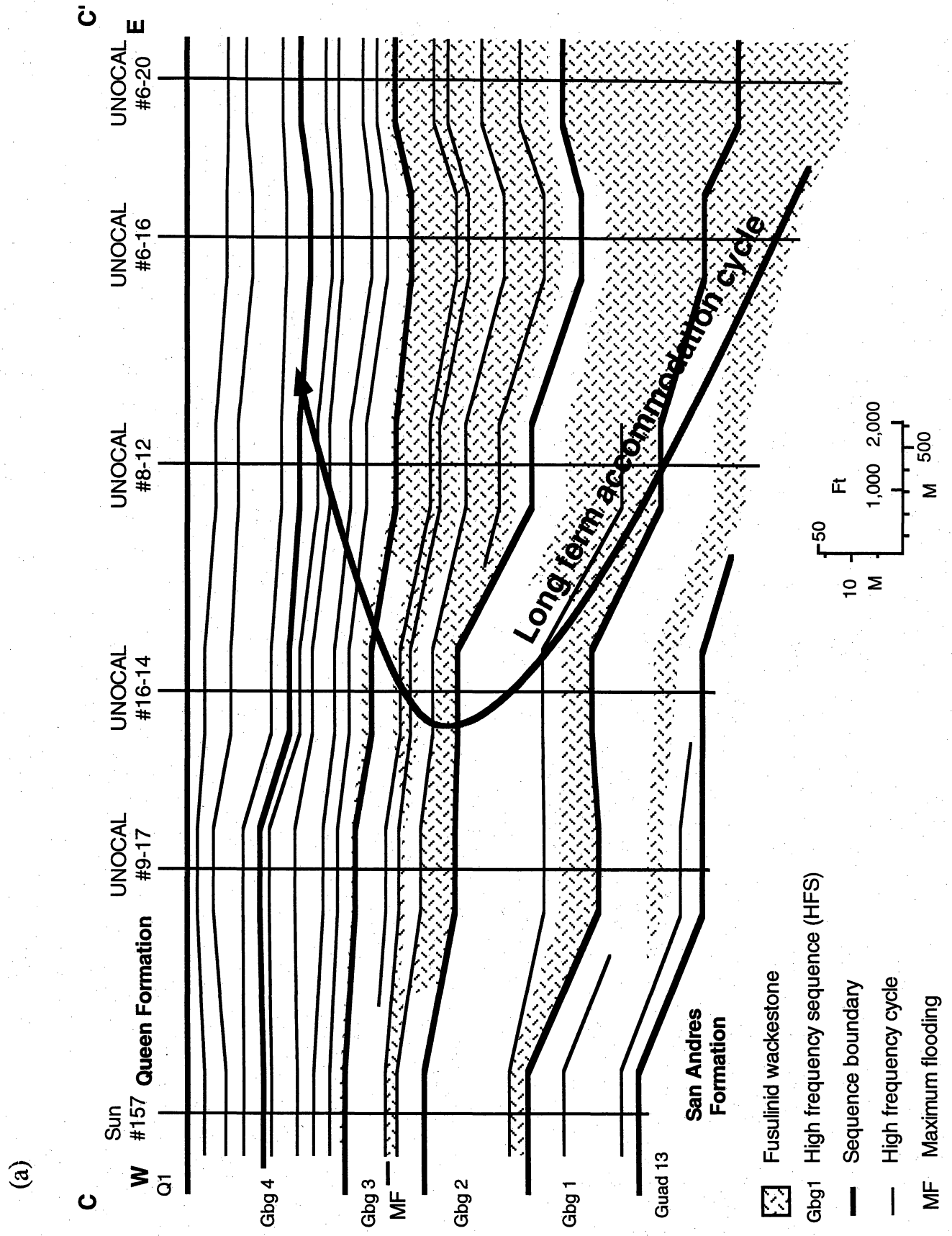

Figure 15. West-to-east, platform-to-basin cross sections detailing high-frequency sequence stratigraphy and the distribution of paleoenvironmentally significant facies in the Grayburg Formation at South Cowden field: (a) fusulinid wackestone facies, (b) grain-dominated packstone-grainstone facies, (c) tidal-flat facies, and (d) sandstone-siltstone facies.

(b)

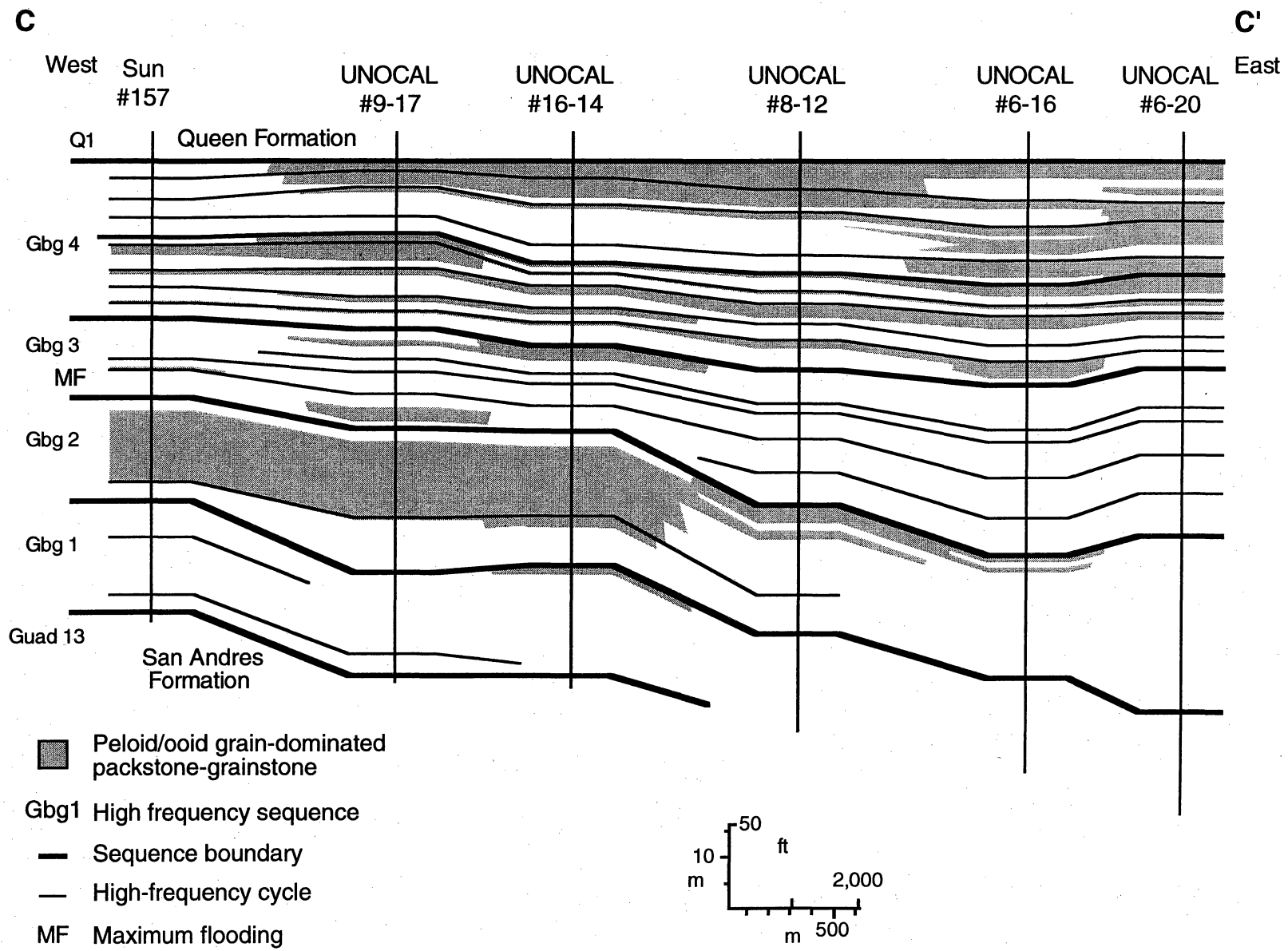

Figure 15 (cont.)

(c)

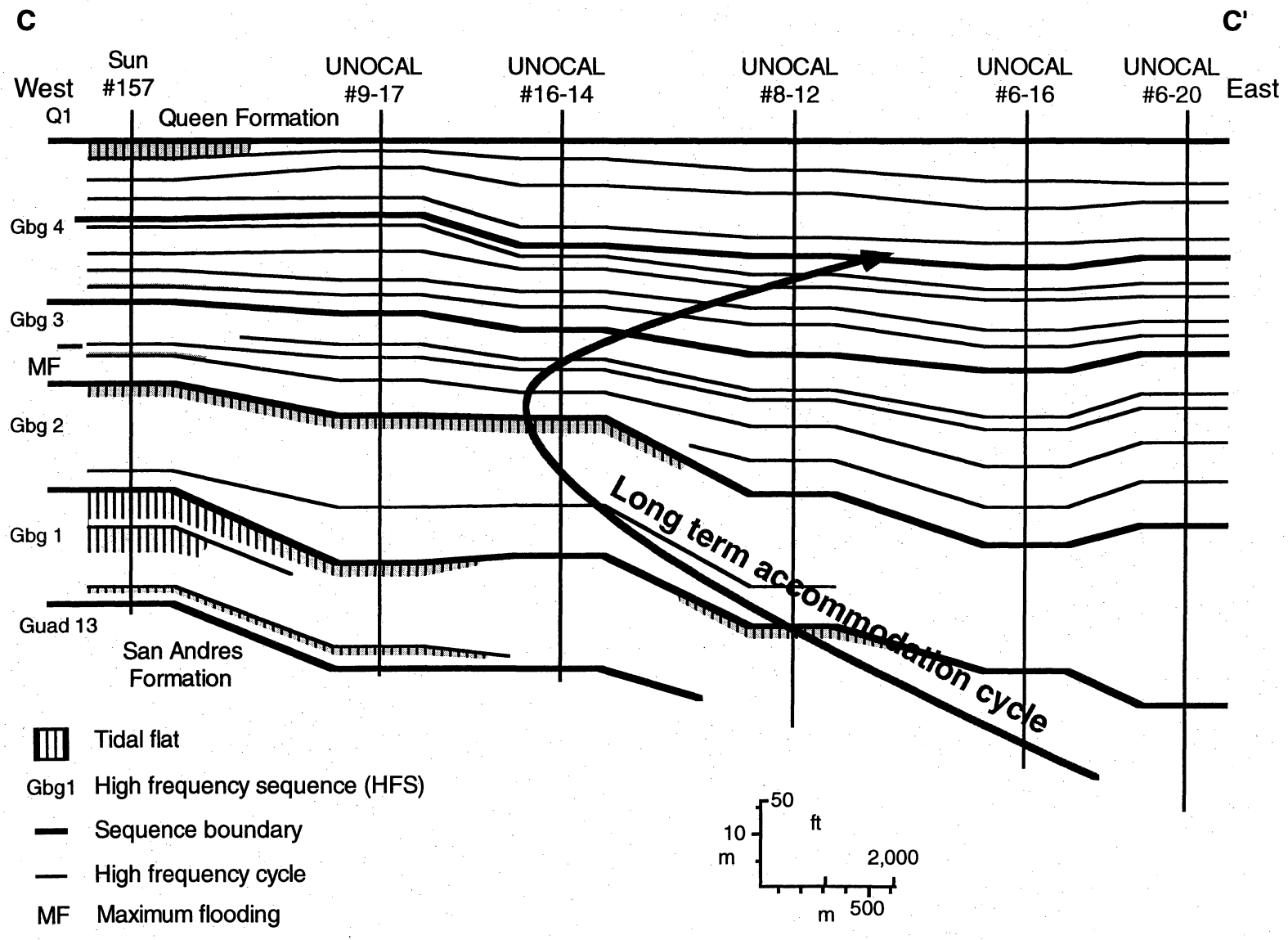

Figure 15 (cont.)

(d)

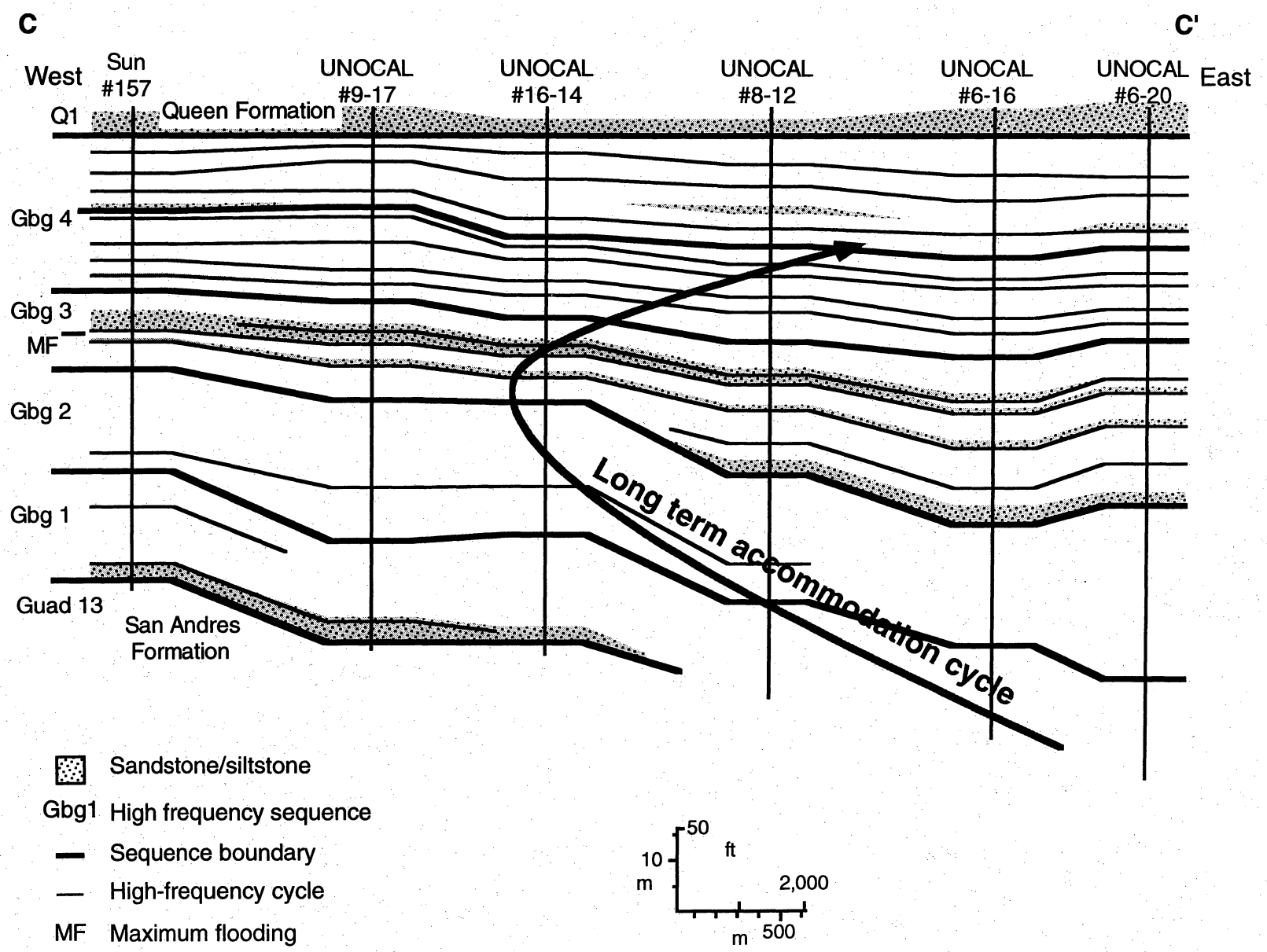

Figure 15 (cont.)

abundance of pore-filling sulfate. Where sulfate is absent from fusulinid molds, porosity may be high but permeability remains generally low. Where complete removal of sulfate, including intercrystalline poikilotopic sulfate, has taken place, both porosity and permeability may be high.

Previous studies have suggested that the optimal growth of fusulinids occurs in no more than 30 ft (10 m) of water (Sonnenfeld, 1991). Downslope transport on the outer ramp appears to extend their depth range to as much as 200 ft (60 m) (Kerans and others, 1994). Empirical observations in South Cowden field and in other Grayburg fields along the Central Basin Platform (Kerans and others, in press) suggest that fusulinid-bearing rocks define maximum water depths in most San Andres and Grayburg reservoir successions. Accordingly, the distribution of fusulinid facies in vertical section is a powerful tool for establishing temporal changes in water depth. As such, the distribution of fusulinids, a deep-water indicator, and tidal-flat facies, an indicator of exposure conditions, are perhaps the two most important facies components for establishing the sea-level history and a basis for time stratigraphic correlations in these reservoirs.

Grain-Dominated Packstone-Grainstone

The term "grain-dominated packstone" is used here for grain-supported rocks that contain at most only slight quantities of carbonate mud. As such, they contain open or cemented interparticle pore space. Those that contain little or no mud and display crossbedding are referred to as grainstones. Two intergradational types of grain-dominated packstone are present in the South Cowden Grayburg. Peloid grain-dominated packstone consists primarily of well-sorted, structureless peloids that range in size from about 90 to 150 microns. Most peloids are probably indurated fecal pellets and poorly preserved ooids. Locally, and especially near the top of HFS 2 and HFS 4 (fig. 15b), there are also intervals of ooid grain-dominated packstone and grainstone. Ooids typically display concentric internal laminations, are well sorted and can be as large as 250 microns. Intervals of ooid grain-dominated packstone do not appear to have significant lateral continuity. Grainstones, both ooid and peloid, are similarly irregular in their distribution,

although like ooid grain-dominated packstone, they are most common in the upper parts of HFS 2 and HFS 4 (fig. 15b).

Grain-dominated packstone and grainstone are most abundant as cycle-capping facies in the tops of longer term accommodation cycles. They are especially common in high-frequency sequence highstand successions at the top of HFS 2 in the western and central parts of the field and in HFS 4 across the field (fig. 15b).

Throughout much of the field, the interparticle pore structure of grain-dominated packstone and grainstone is filled with anhydrite. Where sulfate is absent, however, these rocks develop high porosities and permeabilities. Sulfate nodules are rare in these deposits.

Grain-dominated sediments represent deposition in relatively high energy conditions. Previous studies have interpreted the grain-dominated sediments as representing tidal channels or bars (for example, Bebout and others, 1987; Ruppel and Cander, 1988b).

Peloid Wackestone/Packstone

These deposits contain variable amounts of peloids and significant quantities of carbonate mud. Because virtually all mud-dominated rocks in these successions are bioturbated and pelleted to some extent, and because carbonate diagenesis has obscured original textural characteristics, distinction of mud support and grain support in these peloidal rocks is problematical. Peloids in these rocks range in size from 40 microns to about 120 microns. Skeletal debris, most typically mollusk fragments, but also locally pelmatozoans, is locally common. These rocks are most abundant in HFS 1 in the middle and updip parts of the field and in bases of highstand cycles in HFS 4 in the center of the field (fig. 14).

Especially notable in this facies is the presence of common vertically burrowed zones. These zones are characterized by vertically elongate zones of lighter colored, generally more coarsely crystalline dolomite in a matrix of skeletal or peloidal wackestone. Burrowed zones are commonly associated with vertical strings of anhydrite nodules. Although outlines are diffuse, burrows appear to be about 4 to 6 cm in diameter and up to 30 cm in length. This type of fabric

development is largely restricted to this facies, although locally it is present in fusulinid wackestones. Sulfate is also present in the form of poikilotopic and intercrystalline cement.

Skeletal Wackestone-Packstone

Skeletal wackestone-packstone and peloidal wackestone-packstone are intergradational and difficult to rigorously separate. Both are burrowed and contain ubiquitous peloids and skeletal debris; these rocks, however, contain a higher ratio of skeletal grains to peloids. In the upper or highstand-dominated part of the Grayburg succession (HFS 4) skeletal material is principally mollusk debris, although dasycladaceans are locally present. Pelmatozoans are common in the lower part of this interval. Typically, these deposits are developed at bases of high-frequency cycles that contain higher energy, more grain-dominated facies at their tops. Sulfate is less common in these rocks than in other facies, but it is locally present as small nodules and poikilotopic cement.

Tidal-Flat Facies

The term tidal flat is restricted in this report to those rocks that display features typically associated with subaerial exposure and to those deposits that are intimately associated with the rocks. Included here are fenestral mudstones, cyanobacterial (stromatolitic) laminites, pisolitic mudstones, featureless mudstones, and intraclast breccias, all of which are common in the Grayburg Formation at South Cowden field. Typically, these rocks are devoid of body fossils and burrows are rare. Excluded are clearly subtidal rocks such as those that contain normal marine fossils or those that are extensively burrowed, although such deposits clearly do form in modern tidal-flat environments. The purpose in this usage is to draw attention to those rocks that have water depth significance. Tidal-flat facies in this report represent the shallowest marine deposits in the Grayburg succession. Accordingly, they, like fusulinid deposits, the deepest water assemblage, have important sea-level-history significance.

The inclusive term *tidal flat* is also used for these rocks because both outcrop and reservoir studies have shown that component facies have extremely short correlation lengths. Thus, correlations of tidal-flat textures and fabrics are impossible at any but the finest outcrop scale.

Some systematic variations in tidal-flat fabrics seem likely, however. Kerans and Fowler (1995) suggested that teepee-bearing, pisolitic tidal flats are more abundant in the lower, transgressive parts of long-term accommodation cycles than at their more regressive tops. Fenestral and cyanobacterial mudstones are common in either setting. Similar relationships appear to hold in the South Cowden field area.

Like other Permian successions, such as the San Andres (Bebout and others, 1987; Ruppel and Cander, 1988a, b; Kerans and others, 1994) and Clear Fork (Ruppel, 1992), Grayburg tidal-flat deposits are commonly much lighter in color (light gray to cream) than subtidal facies (brown to gray), reflecting their exposure to near-surface oxidizing conditions. Sulfate, typically in the form of anhydrite, is variably abundant in tidal-flat rocks, principally as poikilotopic, intercrystalline cement and as fenestral pore filling. Porosity can be high in Permian tidal-flat rocks (Ruppel, 1992) when fenestral pores have been opened by sulfate leaching. Permeability generally remains very low.

Tidal-flat deposits are observed at the tops of HFS 1, HFS 2, and HFS 3 in the updip (platform interior) parts of the field (fig. 15c). The thickest tidal-flat succession is developed in the western interior of the field in the basal Grayburg transgressive sequence (HFS 1; fig. 15c). The abundance of pisolite fabrics in these rocks is consistent with its position near the base of the long-term rise that marks the beginning of Grayburg deposition.

Sandstone-Siltstone

Most quartz sand and silt in the Grayburg at South Cowden field is present at high-frequency cycle bases in the transgressive leg of the long-term Grayburg accommodation cycle (fig. 15d). Individual sandstone-siltstone beds are commonly persistent over most of the field

area (at least 15 mi^2). The grain size of these siliciclastics spans the silt-sand boundary, ranging from about 40 to 150 microns; most grains are fine sand. This is consistent with grain sizes reported from other studies of Grayburg reservoirs (Bebout and others, 1987). Most beds contain at least 10 to 20 percent carbonate mud. Grains are typically well sorted, subangular to subrounded quartz; feldspar has not been observed. Some successions display parallel laminations, although many are burrowed or structureless.

Volumetrically, sandstone-siltstone is uncommon in the South Cowden area. Higher abundances of siliciclastics are typical in shore Grayburg successions on the Central Basin Platform (CBP) (for example, North Cowden field) and on the Northern Shelf (for example, Jackson-Grayburg field, New Mexico). Outcrop successions in the Guadalupe Mountains contain much more abundant and coarser grained sandstone and siltstone (Barnaby and Ward, 1995).

Porosity in these rocks is typically low and does not contribute materially to reservoir production. This differs from Grayburg reservoirs farther north on the CBP, such as North Cowden field, where higher porosities make these facies a major contributor to oil production.

The good sorting, grain size, and mineralogical maturity of these clastics suggest that they are wind blown. This conclusion is consistent with interpretations by Fischer and Sarntheim (1988) on the origin of these deposits in the Permian Basin. Depositional textures and fabric associations, however, indicate that they were reworked by subaqueous wave processes before final deposition. Their near restriction to transgressive deposits suggests that they may be remobilized aeolian sand-silt that was accessed during high-frequency sea-level rises. They are most abundant at high-frequency cycle bases in HFS 3, which represents maximum flooding of the platform. This suggests that they were remobilized aeolian deposits that were transported basinward during high-frequency sea-level rises. Because of their continuity, they are good markers for cycle correlation in HFS 3.

Other Minor Facies

Mudstones, although locally present in the South Cowden Grayburg succession, are generally rare. This differs from the San Andres Formation, where cycle base mudstones are common and have important petrophysical and flow modeling significance (Kerans and others, 1994).

Intraclast grainstones are found in tidal-flat successions and as high-frequency cycle caps. Locally, they may develop interparticle porosity. However, on the basis of core control, they appear to be discontinuous and uncommon.

GRAYBURG SEQUENCE ARCHITECTURE

Studies of the Grayburg Formation in outcrops in the Guadalupe Mountains confirm that the Grayburg was deposited during one long-term accommodation cycle (Kerans and Nance, 1991). In general, this cycle is characterized by onlapping, abundant fusulinid-bearing high-frequency cycles at the base and ooid grainstone-capped high-frequency cycles at the top (fig. 14). More recent detailed reservoir and regional subsurface studies, however, illustrate that this long-term accommodation cycle contains four high-frequency sequences (sensu Kerans and others, 1994). Preliminary study of the Grayburg in the Brokeoff Mountains (Barnaby and Ward, 1994) supports this scenario.

Detailed study of log and core data in South Cowden field demonstrates at least three scales of cyclicity. A long-duration cycle that constitutes the entire Grayburg comprises four (possibly five) high-frequency sequences that in turn contain high-frequency cycles.

The long-duration accommodation cycle, spanning the entire Grayburg, ranges from about 300 to 400 ft (90 to 120 m) across the field. As shown in figure 14, this cycle is generally characterized by basal, transgressive fusulinid-bearing facies representing sea-level rise and flooding of the San Andres platform, and topmost grain-dominated packstone and grainstone facies representing the late highstand, fully aggraded terminal Grayburg platform.

The character of the basal Grayburg sequence boundary is uncertain in the South Cowden area because no cored wells have penetrated it. The top Grayburg sequence boundary with the overlying Queen Formation, however, is cored in several wells. The base of the Queen is defined as the base of the first of many thick cycle base sandstones that characterize the Queen in this area (fig. 16). Throughout most of the South Cowden field area, the Queen is composed of characteristic 15- to 30-ft-thick (5- to 10-m) cycles that display sandstone bases and tidal-flat caps. This succession represents a significant basinward offset in facies tracts from that of the underlying Grayburg.

Grayburg High-Frequency Sequences

In South Cowden field, the Grayburg can be divided into four, and possibly five, high-frequency sequences (HFS's) that range from about 50 to 100 ft (15 to 90 m) in thickness across the area. High-frequency sequences are defined using various criteria, including (1) facies offsets at sequence boundaries, (2) internal facies stacking patterns, and (3) high-frequency cycle stacking patterns. Single one-dimensional analysis (that is, examination of these relationships in a single well or core) is generally misleading. Best results are obtained with 2-D cross sections parallel to depositional dip or, even better, with 3-D control.

In the South Cowden area, the lower two Grayburg HFS's (1 and 2) document platform flooding and backstepping associated with sea-level rise, whereas HFS 4 demonstrate aggradation of the platform and basinward progradation during sea-level highstand (fig. 14). Maximum flooding of the platform is demonstrated by HFS 3.

Grayburg HFS 1

The basal Grayburg HFS 1 is characterized by 6- to 12-ft-thick (2 to 4 m) cycles of shallow-water carbonates and sandstones. Basal cycles are restricted inner platform cycles composed of basal sandstones and capping tidal-flat facies (fig. 17). These are overlain by progressively more

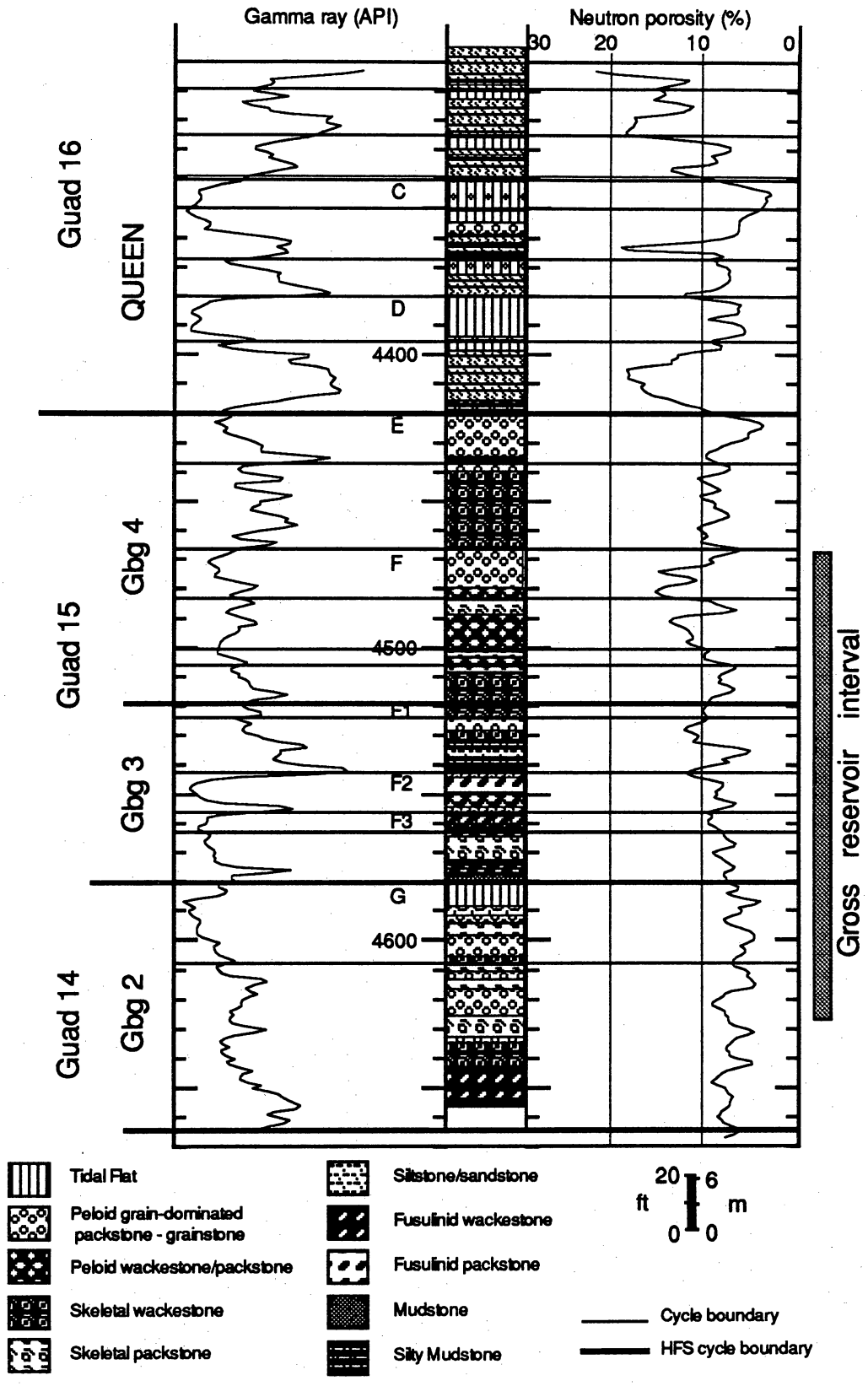

Figure 16. Typical vertical facies succession in the Grayburg and Queen Formations in the western part of the South Cowden Grayburg field, UNOCAL Moss Unit No. 9-17.

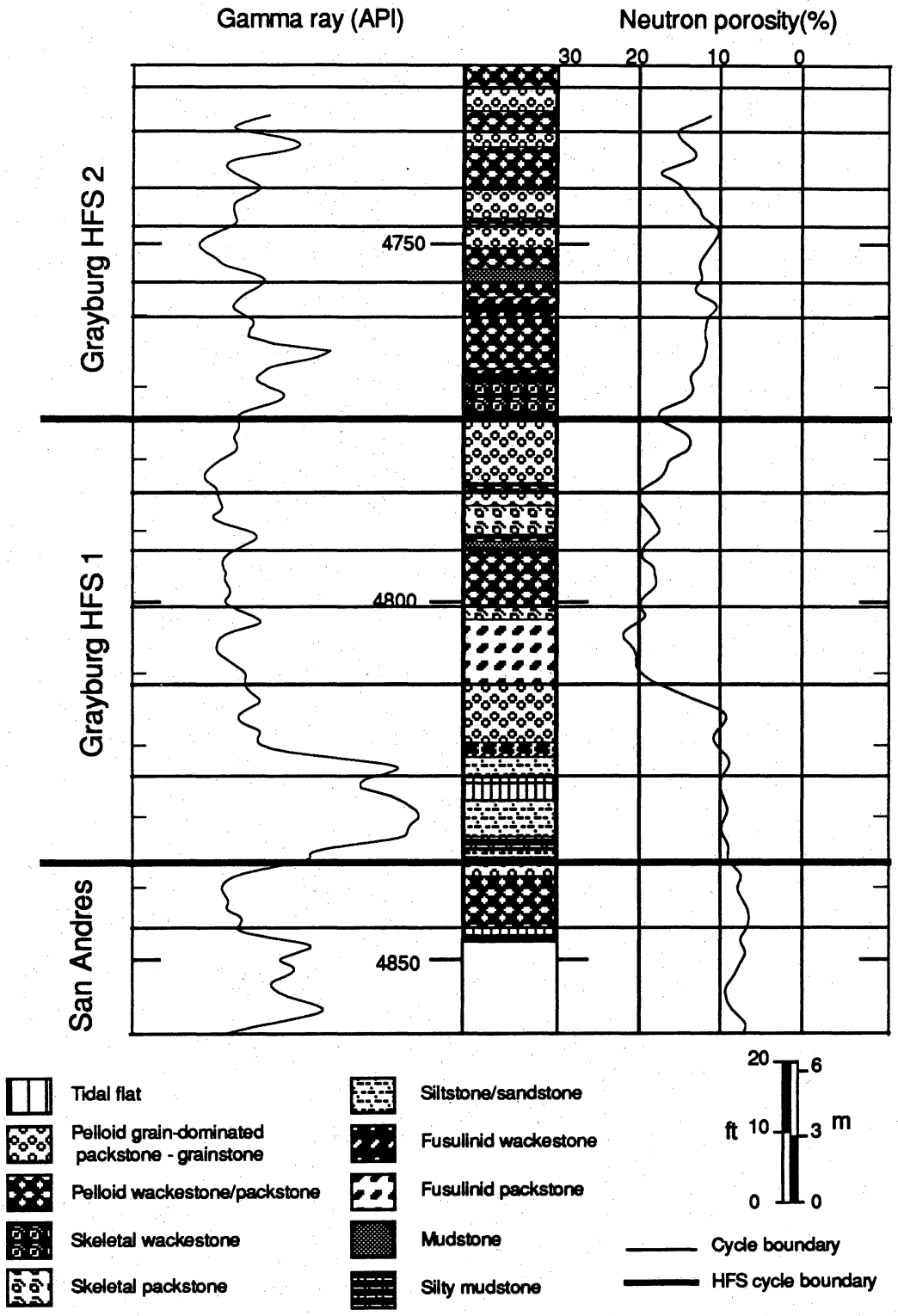

Figure 17. Vertical facies succession in Grayburg HFS 1 in the western, updip part of the South Cowden Grayburg field, UNOCAL Moss Unit No. 13-6.

open marine cycles that document a continued deepening (fusulinid wackestone-based cycles), then a progressive shallowing (cycles capped with peloid grain-dominated packstones). At the western edge of the field, the upper part of HFS 1 is composed of amalgamated tidal-flat cycles, whereas basinward, to the east, HFS 1 comprises fusulinid wackestones (fig. 14). The continuity of high-frequency cycles is difficult to assess because of the scarcity of cores and wireline logs. Available data do not demonstrate laterally continuous cycles.

Grayburg HFS 1 represents the initial flooding of the San Andres platform and comprises backstepping cycles at the base and aggradational, possible outer ramp crest cycles at the top. Limited core data at the Grayburg/San Andres contact suggest that basal Grayburg deposits overlie restricted (inner platform) San Andres deposits updip and open ramp (fusulinid wackestones) downdip. This implies a significant platform-to-basin relief on the San Andres surface in the South Cowden field area at the onset of Grayburg deposition, which was probably inherited from the antecedent topography of the lower San Andres lowstand progradational wedge (Brushy Canyon). Paleotopographic reconstruction of the platform at the end of HFS 1 shows this relief as a southeast-elongate ramp crest surrounded by the deeper water outer ramp (fig. 18). The overall thickness of HFS 1 is about 70 to 100 ft (20 to 30 m) across the field area.

Grayburg HFS 2

More extensive flooding during HFS 2 is indicated by the presence of fusulinid facies at the base of HFS 2 across the entire field area (fig. 14). Even the inner platform tidal-flat complex in the northwestern part of the field was inundated (fig. 14). Juxtaposition of relatively deep water fusulinid facies over tidal-flat deposits suggests a minimum sea-level rise of at least 30 ft (10 m). Early Grayburg paleotopography reflects the strong influence of the underlying lower San Andres progradational lowstand wedge.

The upper, or highstand, leg of the HFS 2 records development of a thick succession of tidal-flat-capped pellet/ooid grain-dominated packstone and grainstone across the area

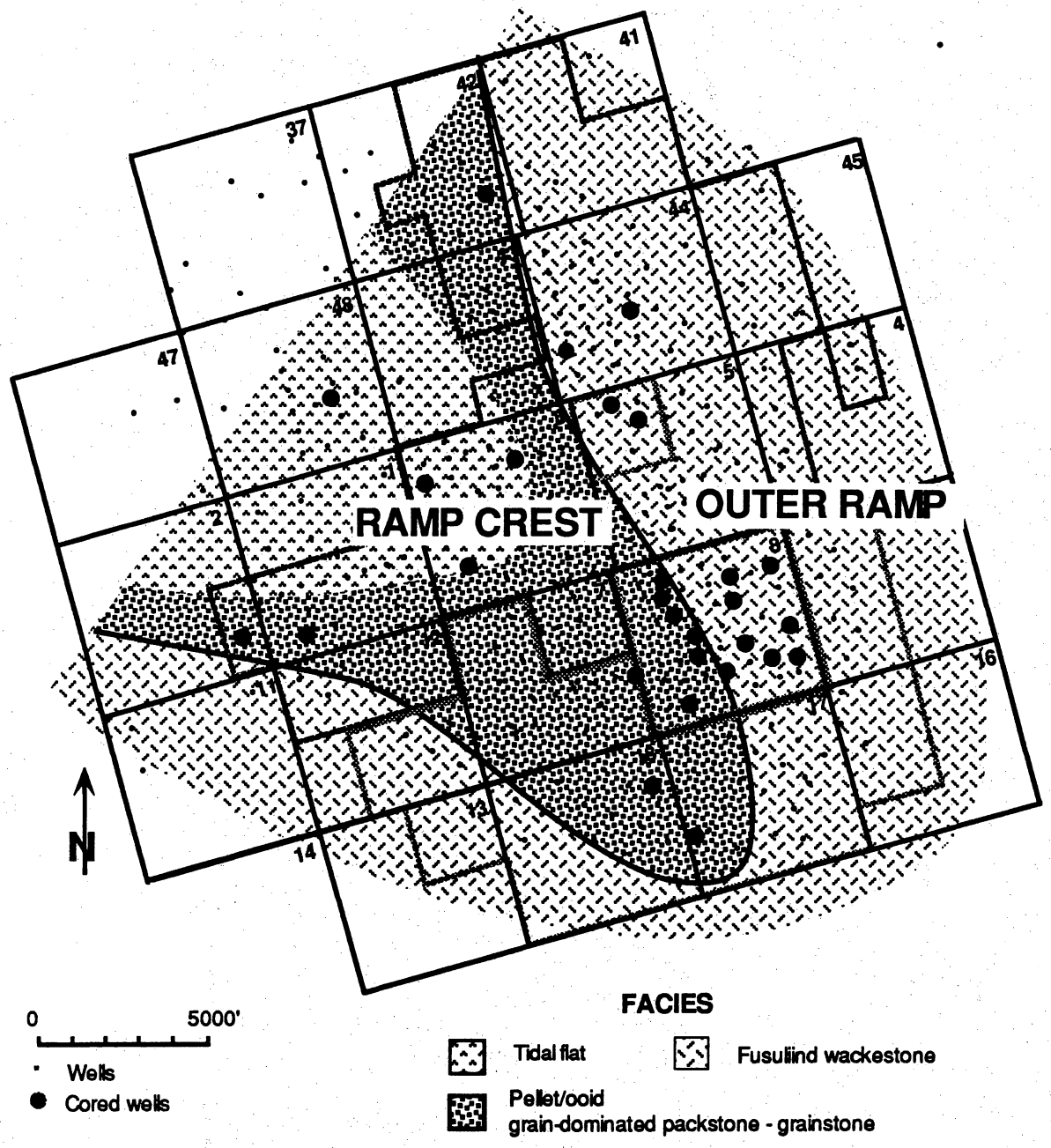

Figure 18. General paleotopography at the end of HFS 1 in the South Cowden field area. The ramp crest is characterized by amalgamated tidal-flat deposits toward the platform and pellet/ooid sands on its outer margins. Note that paleotopography follows the trend of the underlying lower San Andres progradational wedge.

representing the platform ramp crest (figs. 14 and 19). The inner part of the ramp crest is characterized by thick, amalgamated tidal-flat successions.

In high-energy parts of the ramp crest, high-frequency cyclicity is for the most part weakly defined. Neither facies stacking patterns derived from core study nor wireline-log character permit correlation of high-frequency cyclicity. Cyclicity is better developed on the outer margins of the ramp crest (fig. 20) where 10-ft (3-m) cycles with basal wackestones and packstones and capping peloid/ooid grain-dominated packstone and grainstone are correlative for distances of at least 2,000 ft (600 m). These cycles are also correlative on gamma-ray logs (cleaner gamma-ray signatures defining cycles tops) (fig. 20). Cyclicity is also well developed in lower energy, shoreward areas of the ramp crest (fig. 17). Areas of recognizable high-frequency cyclicity are unusual, however. For the most part, high-frequency cycles are not definable in Grayburg HFS 2. This suggests that the internal geometry of these ramp crest grain-dominated packstones and grainstones is complex. Current studies of equivalent Grayburg successions in the Brokeoff Mountains indicate that these deposits are extremely heterogeneous. Barnaby and Ward (1995) showed that grain-dominated successions in Grayburg HFS 2 comprise complex channels that make recognition and correlation of high-frequency cycles difficult.

High-frequency cyclicity in the outer ramp portion of HFS 2 is similarly poorly defined. Although core successions locally display repeated variations in fusulinid content, these "cycles" do not have consistent log signatures and thus are not correlative, at least at the scale of adjacent wells (typically 1,000 to 1,500 ft [300 to 450 m]).

Figure 19, which is based on described cores in the field, gives a general picture of the paleotopography of the Grayburg platform at the end of HFS 2. Perhaps a more accurate depiction is available by considering accommodation trends in the overlying basal HFS 3. Figure 21 displays the thickness trends in the basal accommodation cycle of HFS 3. Areas of major thickness change (20 to 40 ft) define a significant change in relief that probably represents the edge of the ramp crest. Thickness trends in fusulinid facies in HFS 2 are consistent with this pattern (fig. 22), as are facies distribution patterns in the HFS 2 ramp crest (fig. 19).

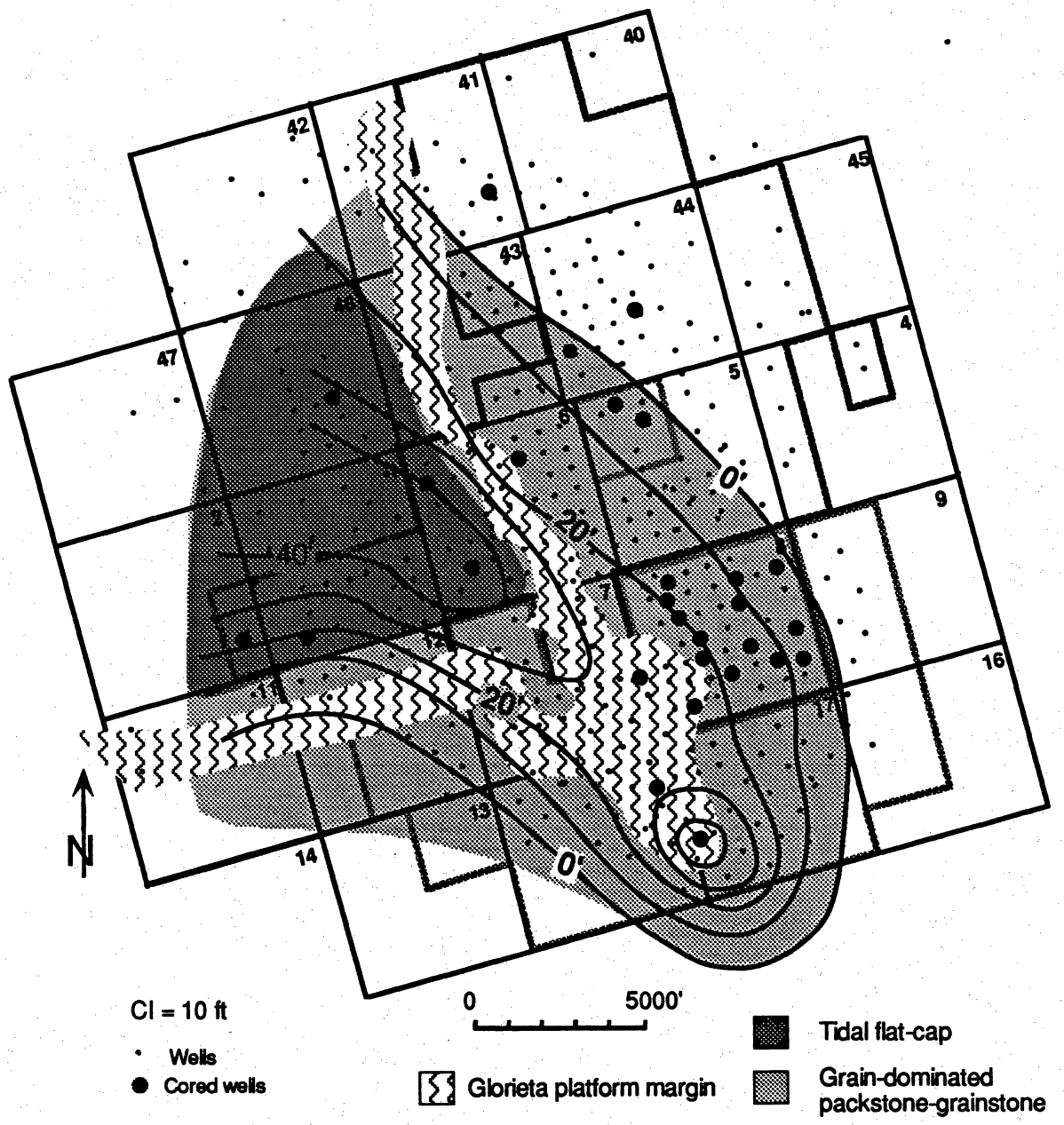

Figure 19. Thickness of grain-dominated packstone and grainstone in the highstand leg of Grayburg HFS 2. Thick amalgamated tidal-flat succession characterize the northwestern part of the area. The position of the ramp crest margin is based on accommodation trends in the over basal HFS 3 (see fig. 21).

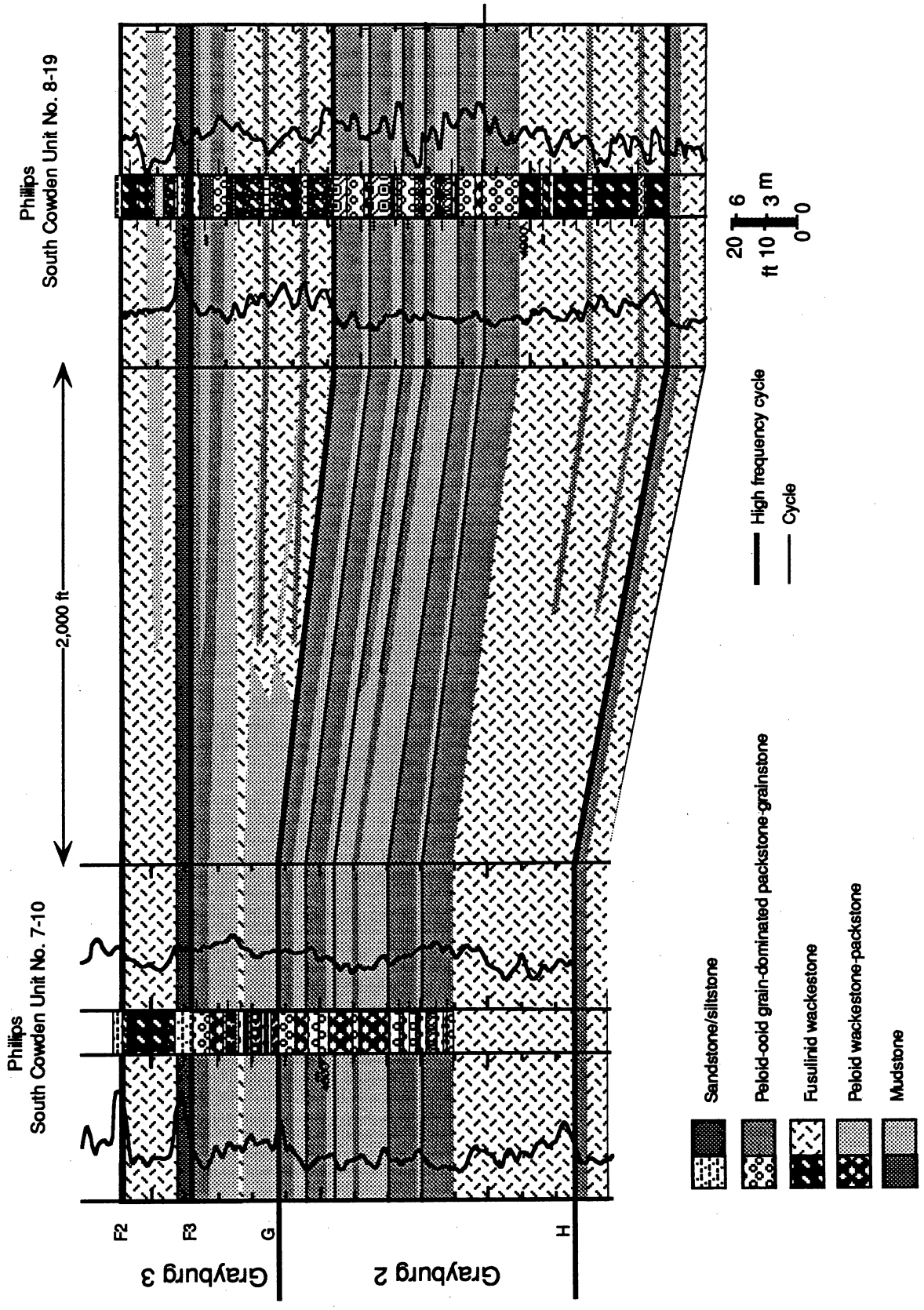

Figure 20. Development of high-frequency grain-dominated packstone-grainstone cycles on the outer margin of the ramp crest (Grayburg HFS 2). See fig. 3 for location of cored wells.

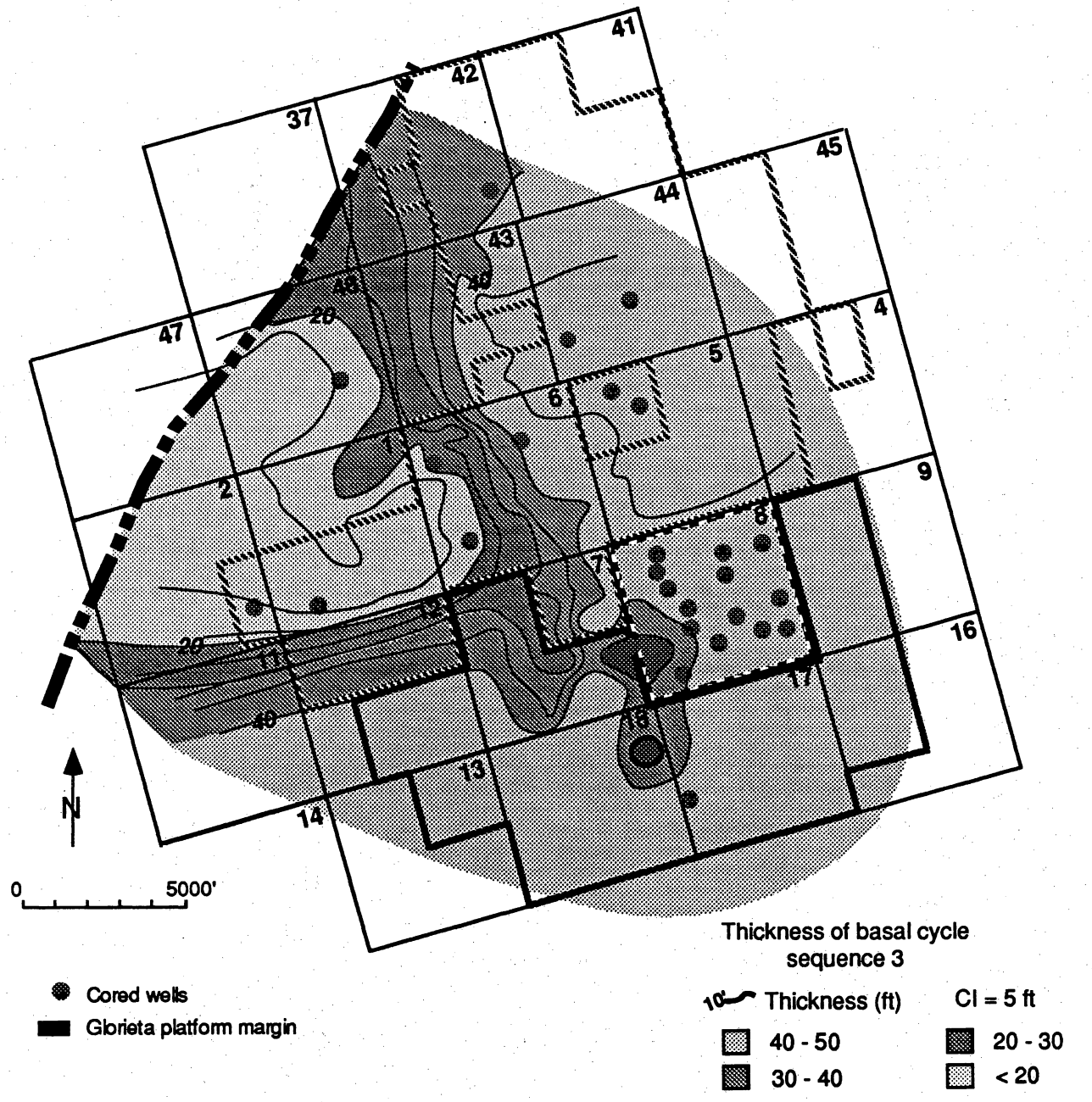

Figure 21. Thickness trends in the basal accommodation cycle of Grayburg HFS 3. The position of the edge of the HFS 2 ramp crest margin is marked by more rapid changes in thickness.

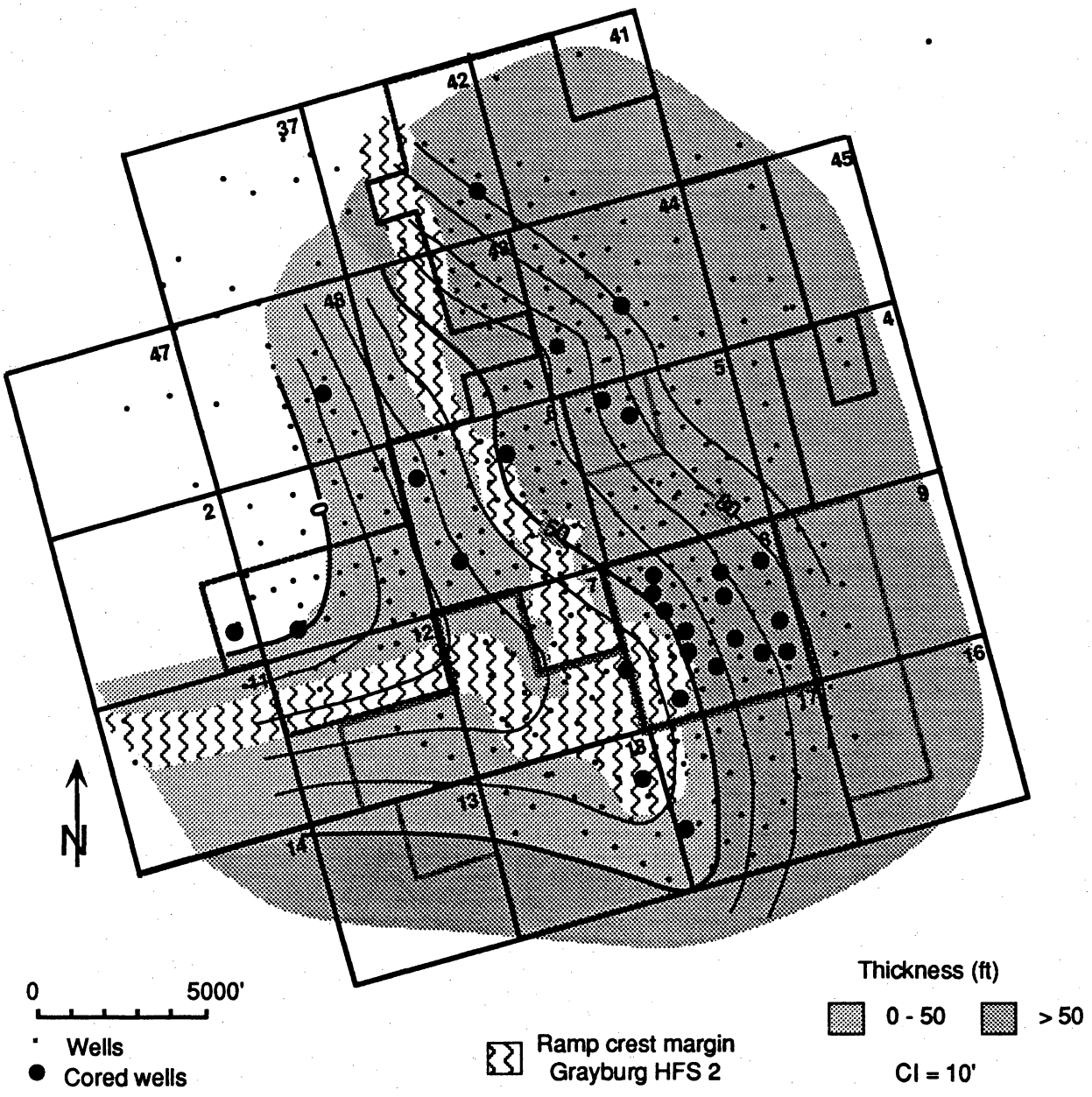

Figure 22. Thickness of fusulinid facies in HFS 2. Thickness trends define the paleotopography of the platform during early Grayburg deposition. Thicknesses based on core data. Also shown is the top of the HFS 2 ramp crest.

Variations in facies composition suggest varying energy conditions along the ramp crest. Whereas the ramp crest succession along the eastern margin of the crest comprises stacked, nearly amalgamated and mud-free ooid/peloid grainstones and grain-dominated packstones (fig. 14), the successions along the south-facing western margin of the crest are more mud-dominated (figs. 17 and 20). This may reflect differences in energy caused by prevailing longshore winds. Fischer and Sarntheim (1988) interpreted geological data from the Permian in the Permian Basin to indicate that prevailing winds were primarily northeasterly (present north) in this area. Such wind trends could account for more energetic reworking and winnowing of ramp crest carbonate sands on the eastern margin of the crest and more restricted conditions on the southern, more leeward margin of the crest (fig. 23).

Total thickness trends in HFS 2 show a general increase basinward in accommodation (fig. 24). Water depth at the end of HFS 2 ranges from exposure on much of the ramp crest to more than 30 ft (9 m) on the outer ramp.

Grayburg HFS 3

Like HFS 2, HFS 3 records a major platform facies offset at its base (fig. 14). Deeper water, outer ramp fusulinid facies extend well up onto the HFS 2 ramp crest. Most evidence indicates that Grayburg HFS 3 documents maximum flooding of the Grayburg platform. This is suggested first by the degree to which outer ramp deposits transgress the platform (fig. 14). Actually, the degree of inundation apparent for HFS 3 from cored wells (fig. 24) is about the same as that documented for HFS 2 (compare figs. 22 and 24). The actual accommodation reflected in HFS 3, measured by thickness of fusulinid facies, however, is greater than that for HFS 2 (compare figs. 22 and 24). Total thickness of HFS 3 ranges from about 40 ft (15 m) in the interior, western part of the field to about 110 ft (33 m) on the downdip eastern margin (fig. 24), a difference of more than 70 ft. Relief on the HFS 2 ramp crest is also illustrated by onlapping basal HFS 3 cycles (fig. 25) .

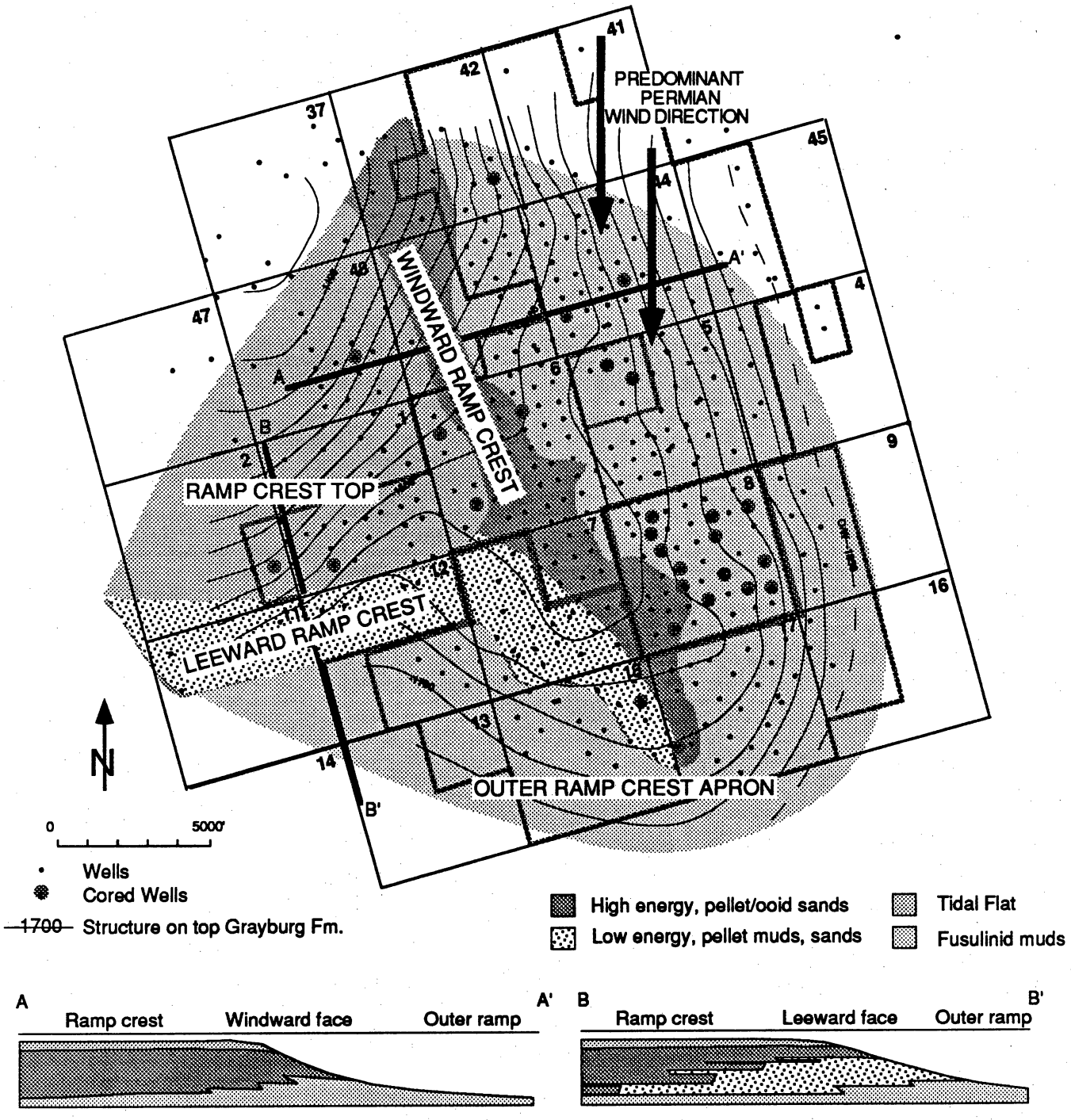

Figure 23. Paleogeography of the South Cowden field area at the end of HFS 2. Prevailing northerly Permian winds may account for higher energy, grain-dominated deposits on the eastern margin of the ramp crest, whereas more mud-dominated sediments accumulated in the leeward, southern margin.

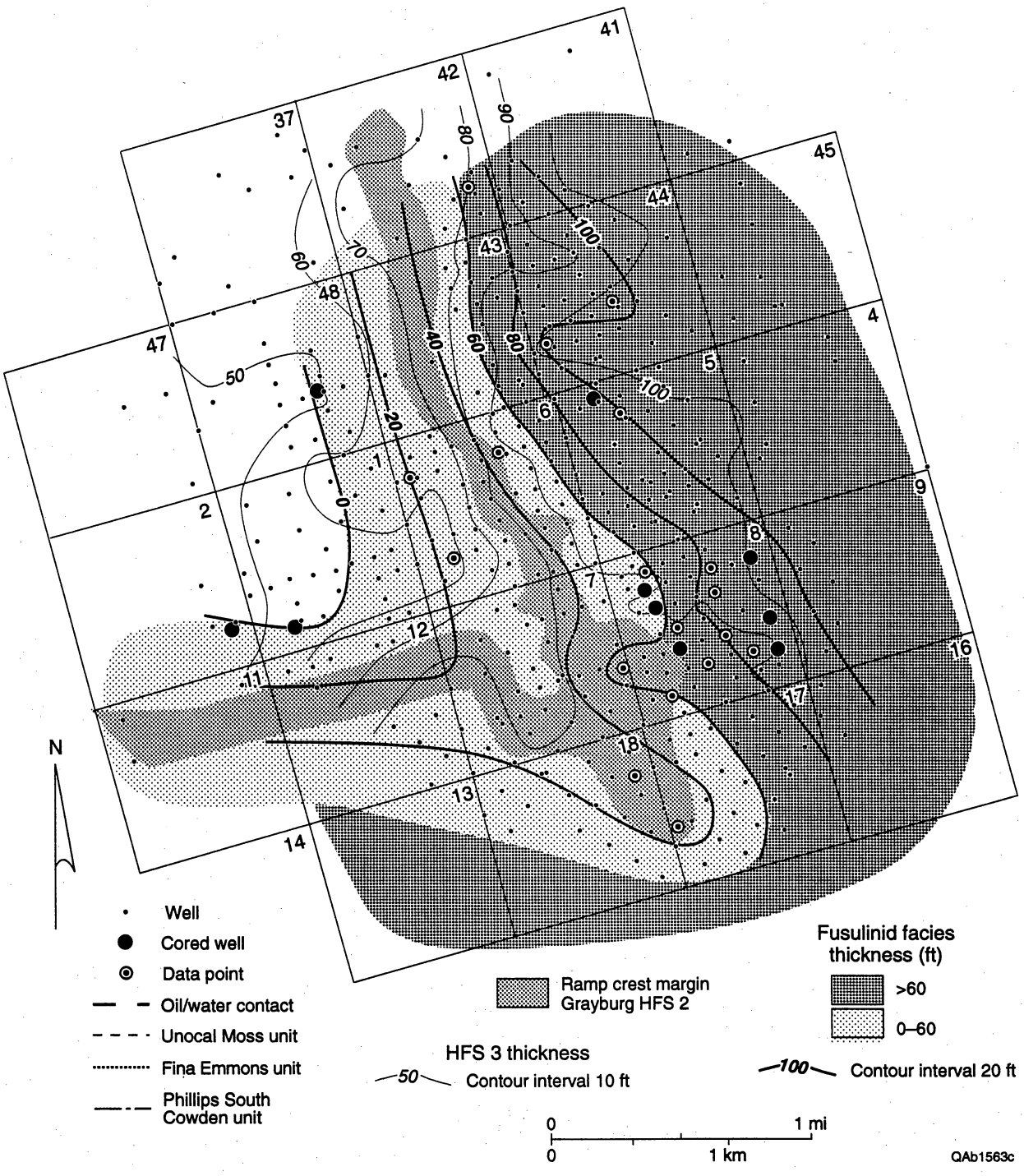

Figure 24. Thickness of fusulinid facies and thickness of Grayburg in HFS 3. Thickness trends show a similar amount of platform inundation, but the overall accommodation created during HFS 3, the maximum flooding sequence, is greater than that evident in HFS 2.

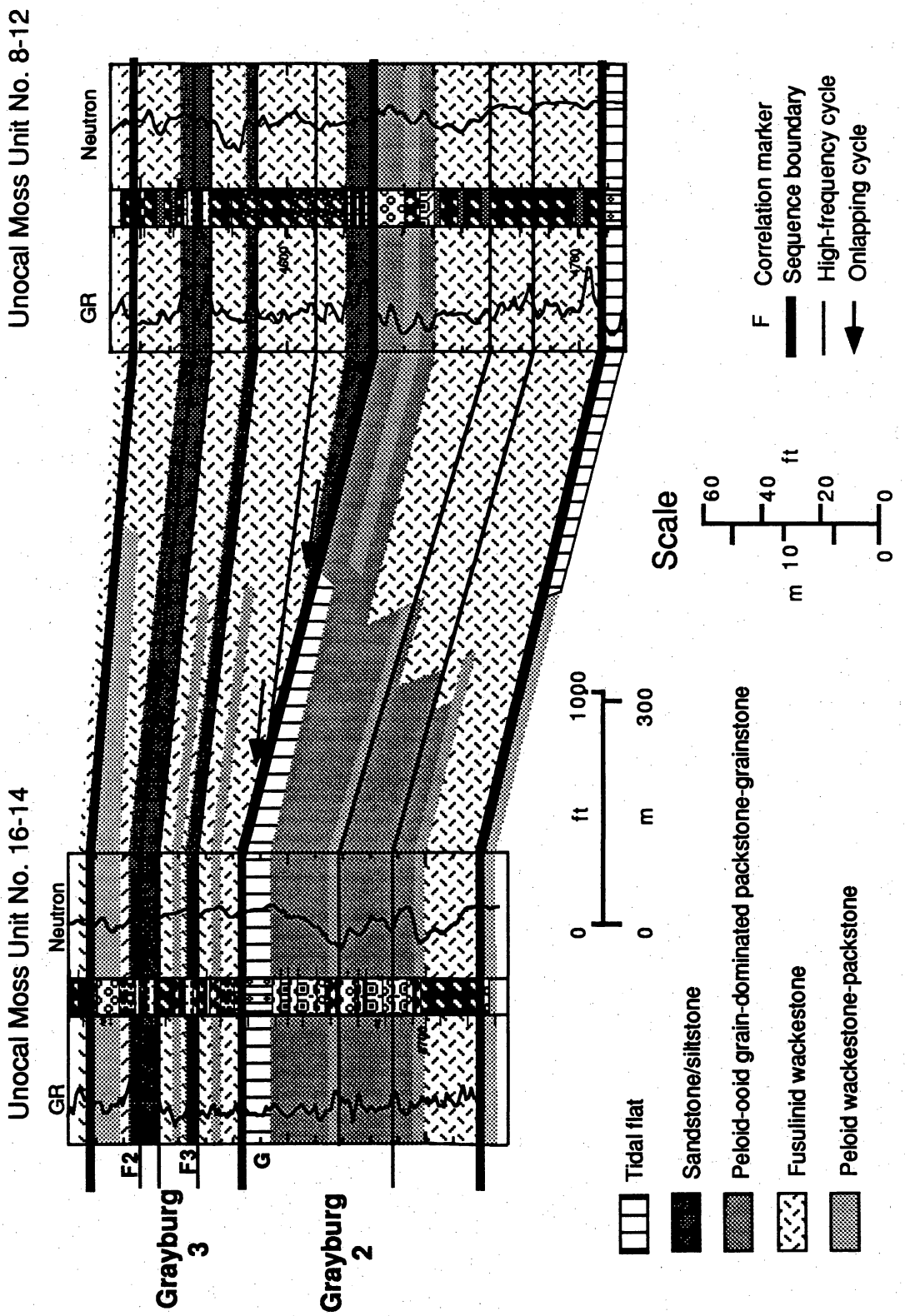

Figure 25. Cross section through the Moss Unit at South Cowden field showing onlap of basal Grayburg HFS 3 on the ramp crest of HFS 2. Siliciclastic-based high-frequency cycles higher in HFS 3 reflect progressively more extensive flooding of the exposed platform and eventual maximum flooding.

Maximum flooding of the platform during HFS 3 is also suggested by the presence of sandstone-siltstone beds (fig. 25). It is probable that these clastics are inner platform aeolian deposits that were reworked by marine waters and delivered to the outer platform as they were inundated. The presence of these clastics at successive high-frequency cycle bases implies the progressive inundation of previously unflooded parts of the platform. Support for this conclusion comes from the observation that siliciclastics in the Grayburg are preferentially deposited in the transgressive legs of cycles both at the cycle and high-frequency sequence scale. In HFS 1, for example, clastics are found at the base of the sequence only as the initial flood back of the platform reached subaerially deposited sands and silts on the platform. Similarly, in HFS 3, clastics are most abundant at the base of the sequence and decrease in abundance upsection across the area, representing a period when more of the interior subaerial platform was inundated. These two sequences appear to mark the bases of two periods of more major platformward flooding; in a sense, they represent the bases of two composite sequences (in the sense that Kerans and others [1994] used the term for the San Andres).

The upper half of HFS 3 documents shallowing on the ramp crest but continued outer ramp deposition to the east (fig. 14). Relief on the platform at the end of HFS 3 appears to have been less than that in lower sequences.

Grayburg HFS 4

Grayburg HFS 4 records the filling of most of the differential accommodation across the South Cowden field area that characterized deposition during Grayburg sequences 1 through 3. Filling also documented by the relatively little change in sequence thickness observed across the area. The lower half of HFS 4 shows a differential accommodation of only about 30 ft (6 m) across the field (fig. 26); the upper half of the sequence displays similar range (fig. 27) but shows no systematic basinward increase in accommodation. Accordingly, much of the sequence contains very similar facies across the area (fig. 14).

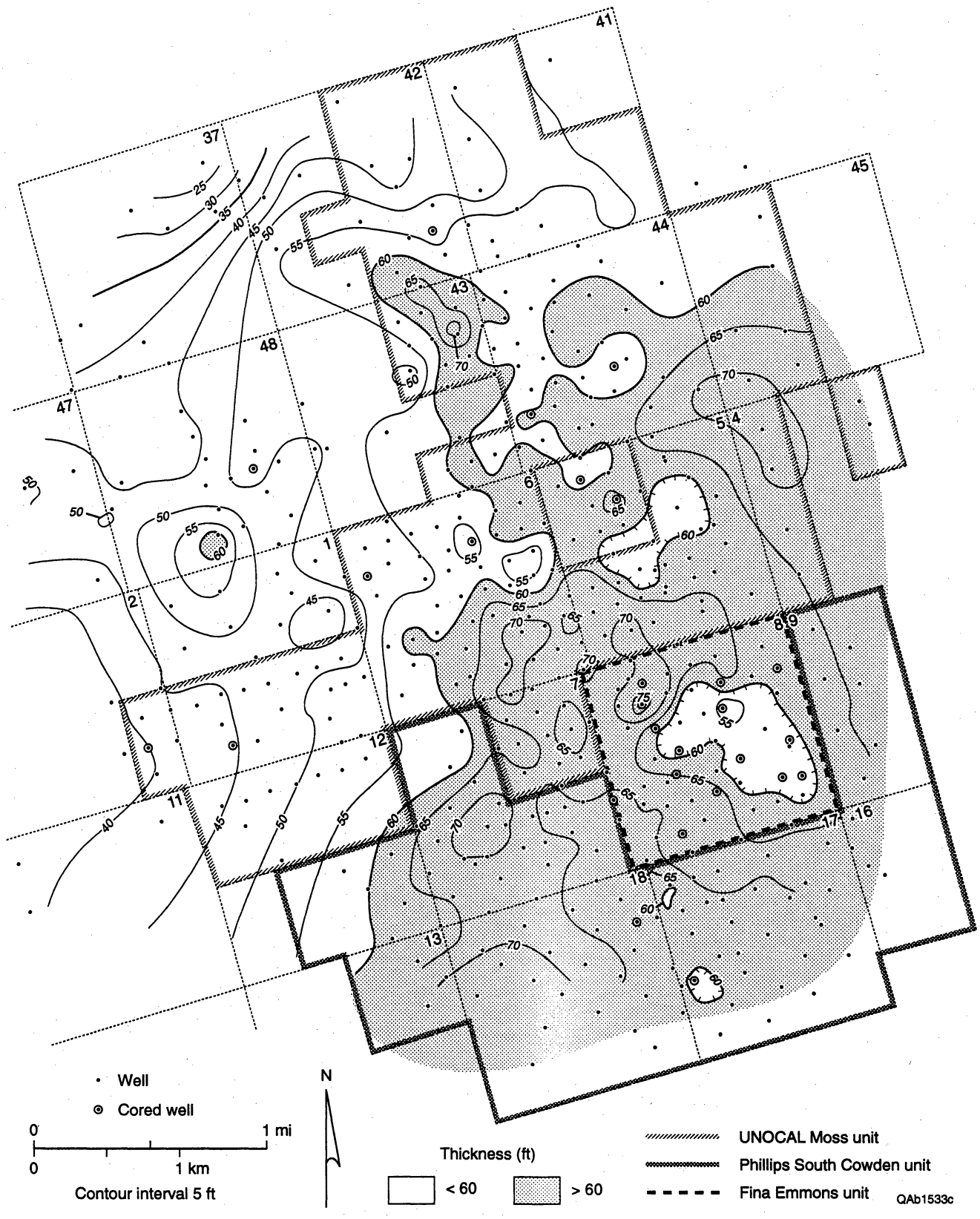

Figure 26. Thickness of the Grayburg lower half of Grayburg high-frequency sequence 4 (HFS 4) in South Cowden field.

Figure 27. Thickness of the Grayburg upper half of Grayburg HFS 4 in South Cowden field.

The contact of Grayburg HFS 4 with the underlying HFS 3 sequence is subtle. Although HFS 4 reflects a major basinward shift in facies tracts, the actual position of the sequence boundary is defined only by a minor flood back, with fusulinid facies extending as a thin veneer across most of the platform (fig. 14). Above these basal fusulinid beds, the rest of the Grayburg consists of highly cyclic, largely aggradational successions of peloid wackestone to grainstones (fig. 14). These deposits indicate that depositional relief across the South Cowden field area was greatly reduced very soon after the beginning of HFS 4 deposition.

As a result of this reduced relief, high-frequency cyclicity is very well expressed in this sequence. Well-developed cycles comprise 10-ft-thick (3-m) successions of basal peloid/skeletal wackestones and mud-dominated packstones and capping peloid/ooid grainstone to grain-dominated packstone (fig. 14). Cycles have persistent log responses and can be readily correlated across most of the field area. The internal facies composition of these cycles varies significantly across the field, however. Many cycles, for example, do not display grain-dominated caps. Some 2-D sections suggest a systematic development of capping higher energy grain-dominated facies. Figure 28, a short dip section in the southern part of the area, for example, shows a basinward shift in the distribution of grain-dominated capping facies; Figure 14, a similar section to the north, shows the same relationship.

The basinward shift in the distribution of higher energy cycles may be evidence of a more subtle high-frequency sequence boundary at this part of the section. The presence of breccias and hardgrounds at the F marker (fig. 28) may also support this interpretation. Apparent basinward-stepping cycles in the lower half of HFS 4 are overlain by what appear to be platform stepping cycles in the upper half of HFS 4 (fig. 14). Outcrop successions of Grayburg HFS 4 equivalents in the Guadalupe Mountains show a similar trend in the distribution of grain-dominated facies (Kerans and Nance, 1991). Correlative sections through Grayburg HFS 4 elsewhere along the Central Basin Platform margin, however, do not show indications of a sequence break at this point. Until further data are available, the possibility of an additional sequence break at this point in the Grayburg section is conjectural.

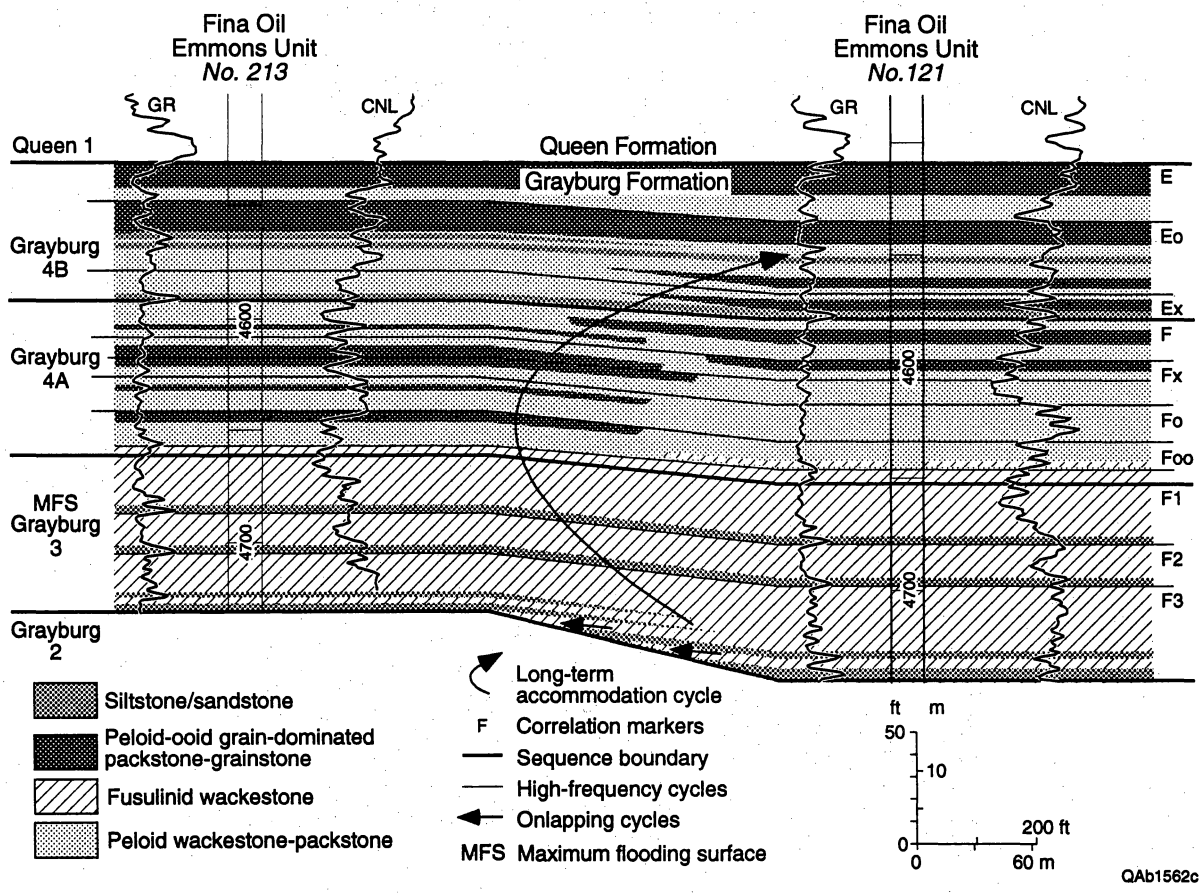

Figure 28. High-frequency cyclicity in Grayburg highstand deposits (HFS 4). See figure 3 for location of cored wells.

The mud-dominated high-frequency cycles of HFS 4 are reminiscent of lower energy cycles developed on the leeward part of the HFS 2 ramp crest; they consist of mud-dominated bases and grain-dominated tops and are highly correlative. By HFS 4 time, however, facies evidence suggests that outer ramp facies had shifted well to the east of the field area. Mapping of thickness trends in HFS 4 illustrates that these cycles were deposited in a leeward setting, toward the shore of the ramp crest (fig. 29). The aggregate thickness of grain-dominated facies in HFS 4 increases to the eastern margin of the field, suggesting that the ramp crest lies in approximately this position.

Discussion

The high-frequency sequence framework of the Grayburg is well constrained along the eastern margin of the Central Basin Platform and in South Cowden field. Key to developing this framework, however, is the construction of multiple platform-to-basin 2-D cross-section panels along the Central Basin Platform margin. Because of differences in structural setting, accommodation and depositional styles vary along strike and along dip. Accordingly, one-dimensional analysis of sequences in individual wells is unlikely to result in an accurate interpretation of sequence framework.

The most obvious event in Grayburg deposition is the major landward facies offset that characterizes maximum flooding during the middle of the Grayburg long-term accommodation cycle. This feature is recognizable in virtually all Grayburg platform carbonate successions in the Permian Basin as a major shift of outer ramp fusulinid facies toward the platform. High-frequency sequences recognized in South Cowden field, however, are variably developed and therefore not always easily definable in all settings. Kerans and Fitchen (1995) assigned two formal sequences to the Grayburg (HFS 14 and HFS 15) on the basis of the position of the major platform flooding event. This two-fold subdivision is particularly obvious in outcrops in the Guadalupe Mountains (Kerans and Nance, 1991). Although the top of Grayburg HFS 14 is well

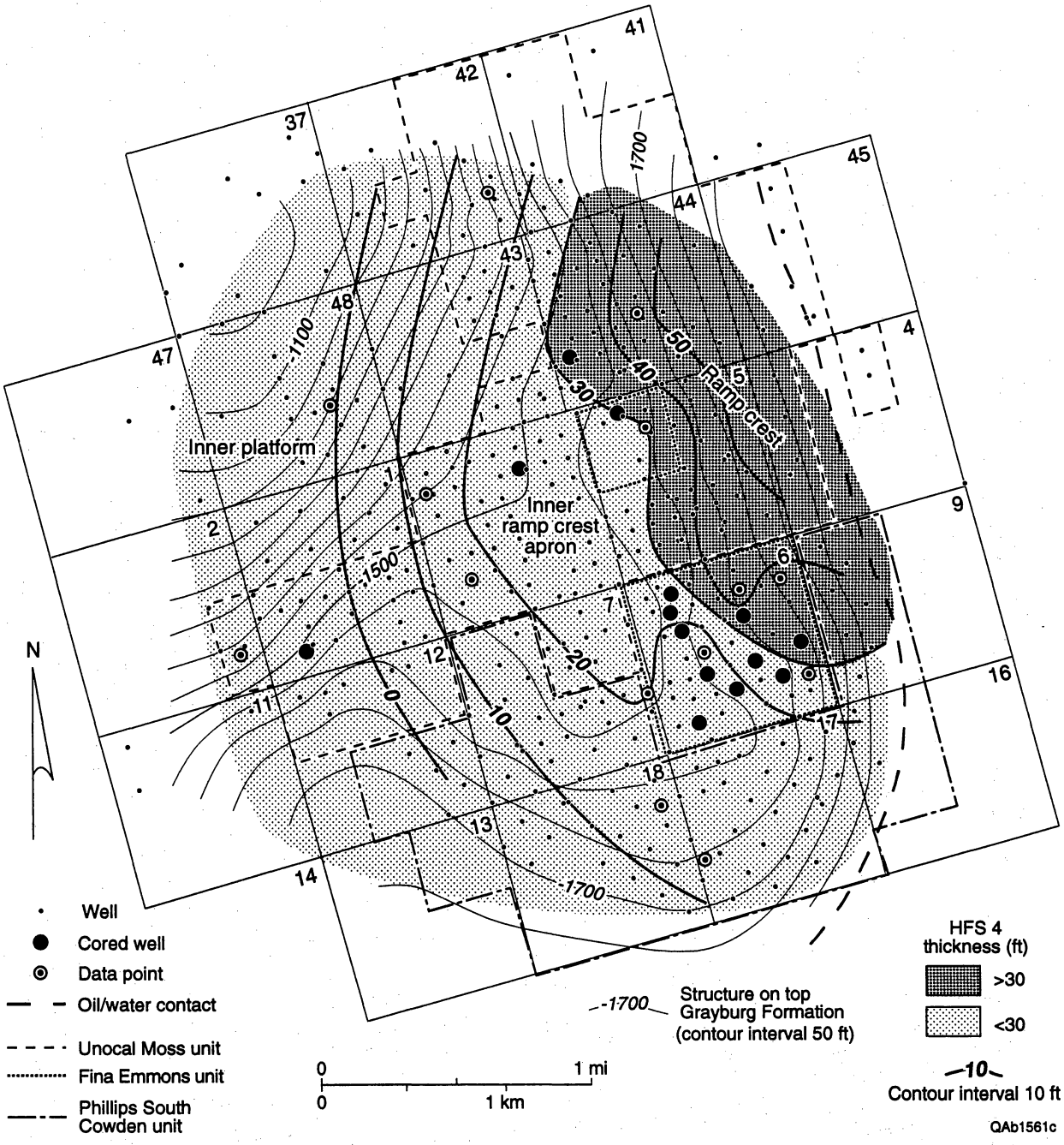

Figure 29. Paleogeography of HFS 4. The position of the ramp crest is inferred from distribution of grain-dominated facies from cored wells.

represented in South Cowden by the well-developed highstand ramp crest at the top of Grayburg 2 (fig. 14), it is not so obvious elsewhere.

Grayburg high-frequency cyclicity is generally definable in the subsurface in ramp crest and inner ramp successions. Low-energy ramp settings seem to produce more contrast in cycle base and cap facies and thus produce a more distinguishable and correlatable log expression. Outer ramp fusulinid successions, on the other hand, do not typically display definitive log signatures except where they contain cycle base sandstones and siltstones. Amalgamated tidal-flat successions are similarly difficult to recognize unless they contain cycle-base siliciclastics.

The three scales of cyclicity expressed in the Grayburg Formation form the basis for a chronostratigraphically defined reservoir framework. High-frequency sequences define major facies tracts and can constrain the disposition of depositionally controlled rock-fabric packages. Recognition and correlation of the Grayburg long-duration cycle forms the basis for correlating and comparing equivalent Grayburg reservoir and outcrop successions throughout the basin. Finally, high-frequency cycles constitute the basis for a high-resolution, flow unit scale subdivision of the reservoir that can form the basis for modeling and simulation. The latter is a powerful tool for defining and mapping depositional facies and derivative rock-fabric heterogeneity.

RESERVOIR FRAMEWORK: SOUTH COWDEN FIELD

Virtually all of the production from South Cowden Grayburg comes from HFS 2–4 in the current study area (fig. 14). The cycle stratigraphic framework presented above forms a basis for subdividing this part of the Grayburg reservoir succession for modeling and simulation. High-frequency highstand cycles in the upper highstand leg of the Grayburg (HFS 4) are continuous and definable throughout most of the South Cowden field study area. We have used these cycles, which average 10-15 ft (3-5 m) thick to subdivide HFS 4 into as many as eight stratigraphic units (fig. 28). For reasons already discussed, however, such high-frequency cycles are not resolvable throughout all of the reservoir. In HFS 3, we used dominantly transgressive sandstone-siltstone-

based fusulinid cycles to divide the sequence into three parts (fig. 28). Because it is dominated by high-energy highstand ramp crest deposits that display inconsistent log signatures and by outer ramp facies that are characterized by poorly organized successions of fusulinid-dominated deposits, HFS 2 does not lend itself to further subdivision on the basis of high-frequency cyclicity.

Overall, the Grayburg succession can be subdivided into 12 architectural units for modeling and simulation. In the most productive part of the reservoir, HFS 3 and HFS 4, these units average 10 to 15 ft (3 to 5 m) in thickness.

GENERAL POROSITY TRENDS

Porosity•thickness maps have been constructed for some of the Grayburg high-frequency sequences and subsequences to examine large-scale trends in porosity development across the field. Although the gross productive interval extends below HFS 3, incomplete well penetration precludes consistent mapping of phi•h in that interval. Total phi•h for HFS 3 and HFS 4, the most highly productive intervals in the reservoir (fig. 30), shows that the highest porosities are developed along the eastern margin of the field. For HFS 3, this corresponds with the position of outer ramp fusulinid facies. During HFS 4, this area was the site of the leeward side of the ramp crest (fig. 29).

Mapping of HFS 3 alone (fig. 31) shows that virtually all of the phi•h is located in outer ramp fusulinid facies. A much less clear-cut association with facies is apparent from the phi•h map of the lower half of HFS 4 (fig. 32). As previously described, all of HFS 4 comprises very similar deposits of stacked, back-ramp, mud-dominated and grain-dominated peloid high-frequency cycles. Thus, the preferred development of porosity in the southern and eastern parts of the field has no apparent relationship to depositional facies or cycle patterns. A better case can be made for the upper half of HFS 4 displaying a relationship between porosity development and facies. Most of the phi•h in the upper half of HFS 4 is developed in the eastern part of the field in the area of the HFS 4 ramp crest (fig. 33).

Figure 30. Phi•h map of the major Grayburg productive reservoir section (HFS 3 and HFS 4).

Figure 31. Phi•h map of Grayburg HFS 3.

Figure 32. Phi•h map of the lower part of Grayburg HFS 4

Figure 33. Phi•h map of the upper part of Grayburg HFS 4.

Cursory comparison of phi•h trends and facies patterns suggests a possible connection between original depositional textures and porosity distribution for several of the major high-frequency sequence packages. A more careful look at patterns of diagenesis in the field, however, suggests that this is an oversimplification.

DIAGENESIS

Like all shallow-water platform carbonate successions in the Permian Basin, the Grayburg reservoir succession in South Cowden field has undergone several types and stages of diagenesis. Most significant among the diagenetic changes that have affected these reservoirs are dolomitization, sulfate emplacement, and sulfate removal.

Several previous studies have published detailed accounts of the diagenetic processes that have affected Guadalupian reservoir successions (for example, Bebout and others, 1987; Ruppel and Cander, 1988a, b; Leary and Vogt, 1990; Longacre, 1990; Major and others, 1990). Perhaps the most important results of these studies have been the conclusions that (1) although some early dolomitization may have occurred (for example, Ruppel and Cander, 1988a, b; Leary and Vogt, 1990), major dolomitization of these rocks probably occurred during the late Guadalupian (Ruppel and Cander, 1988a, b), (2) dolomite has been locally replaced by anhydrite (Ruppel and Cander, 1988a, b; Leary and Vogt, 1990), (3) late removal of sulfate has resulted in porosity enhancement (Bebout and others, 1987; Ruppel and Cander, 1988a, b; Leary and Vogt, 1990; Longacre, 1990; Major and others, 1990; and many others). The Grayburg reservoir at South Cowden field displays characteristics of all of these processes and, perhaps more than other previously studied reservoirs, owes its origin to diagenetic processes.

Two important diagenetic processes—dolomite recrystallization and alteration and leaching of anhydrite—have been documented in other Guadalupian reservoirs and appear to be important to porosity development in the Grayburg reservoir at South Cowden field.

Dolomite Recrystallization

Evidence of dolomite recrystallization is localized in irregular, light-colored (light-brown), vertically elongate zones of altered dolomite fabric (fig. 34). In some cases they strongly resemble vertical burrow tubes of approximately 6-8 cm in width and 20 cm or more in length. Commonly these zones contain vertically oriented strings of small anhydrite nodules. Petrographically, they vary considerably. In most cases, however, they display crystal sizes coarser than the surrounding host rock, which is typically darker in color (brownish gray); matrix crystals average 10 to 30 microns, whereas recrystallized zones average 40 to 80 microns and larger. In many of these intervals, dolomite rhombs have leached cores. Dolomite in recrystallized zones also contains common, relatively inclusion free, rimming cement overgrowths. Both dolomite rims and rhomb centers, when unleached, display relatively uniform, dull red cathodoluminescence.

Recrystallized zones are stratigraphically restricted in their distribution in the upper part of HFS 3 and in the lower part of HFS 4 (fig. 35). They are most developed in mud-dominated facies, including skeletal and peloidal wackestones and packstones. Locally, they are developed in fusulinid-bearing rocks in the upper part of HFS 3. In these rocks, they are most common in peloid-dominated caps to high-frequency, fusulinid-wackestone-based cycles. Recrystallized zones are most common on the outer margins of the field (fig. 36).

Light-colored, recrystallized dolomite zones display significantly higher porosity and permeability than do enclosing darker colored wackestones and packstones. Porosity logs through sections affected by dolomite recrystallization typically show substantial vertical variation in porosity (fig. 37). These variations do not coincide with facies variations in high-frequency cycles but rather appear to reflect the irregular abundance of altered zones through the section. Permeability values from whole-core analysis vary directly with the amount of recrystallized fabric present in each core piece. To document porosity and permeability variations more specifically in these intervals, Phillips Petroleum Company carefully targeted, sampled, and analyzed core plugs from both light-colored, recrystallized dolomite zones and

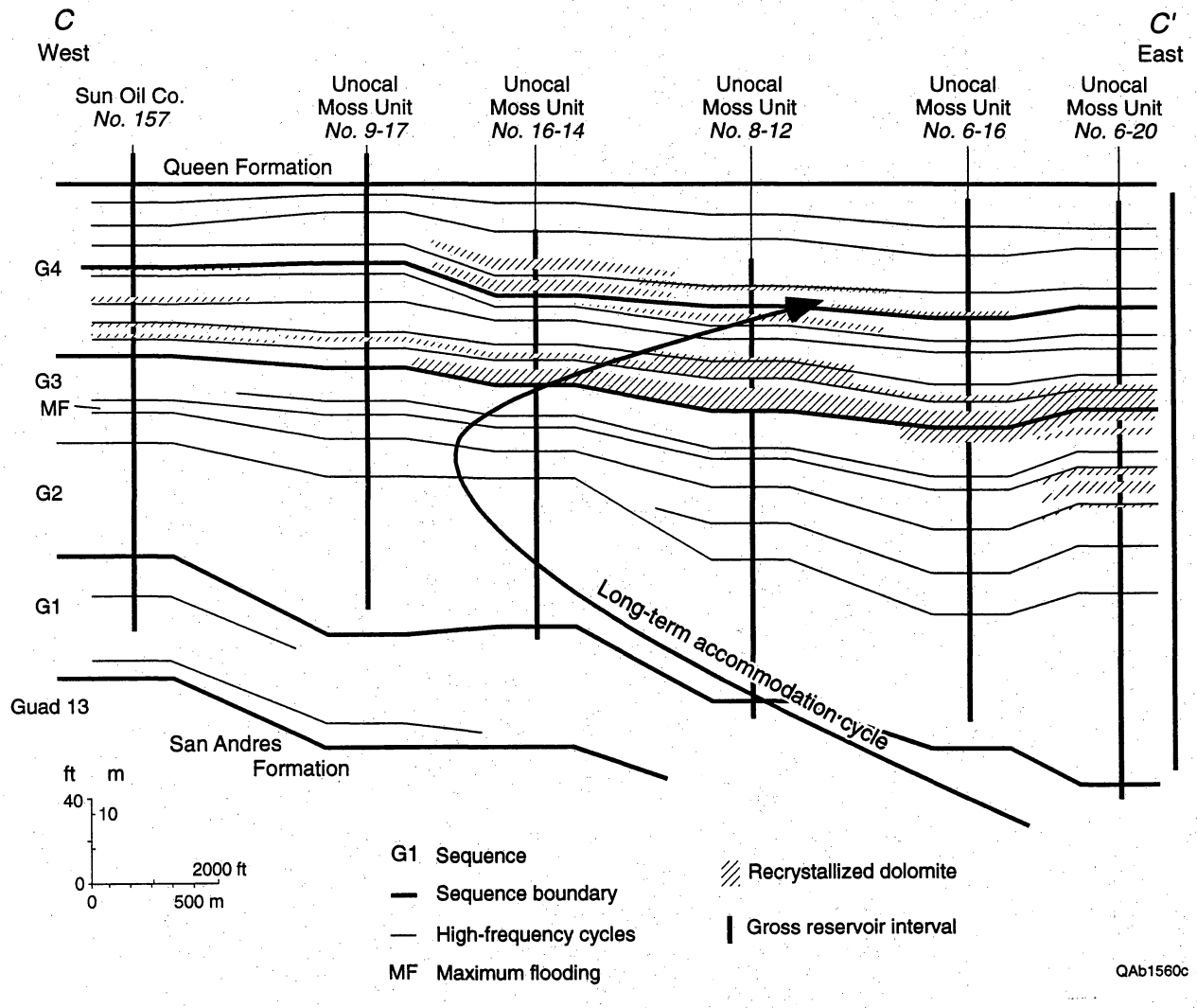

Figure 35. Cross section (C–C′) through the UNOCAL Moss Unit showing the stratigraphic distribution of zones of recrystallized dolomite.

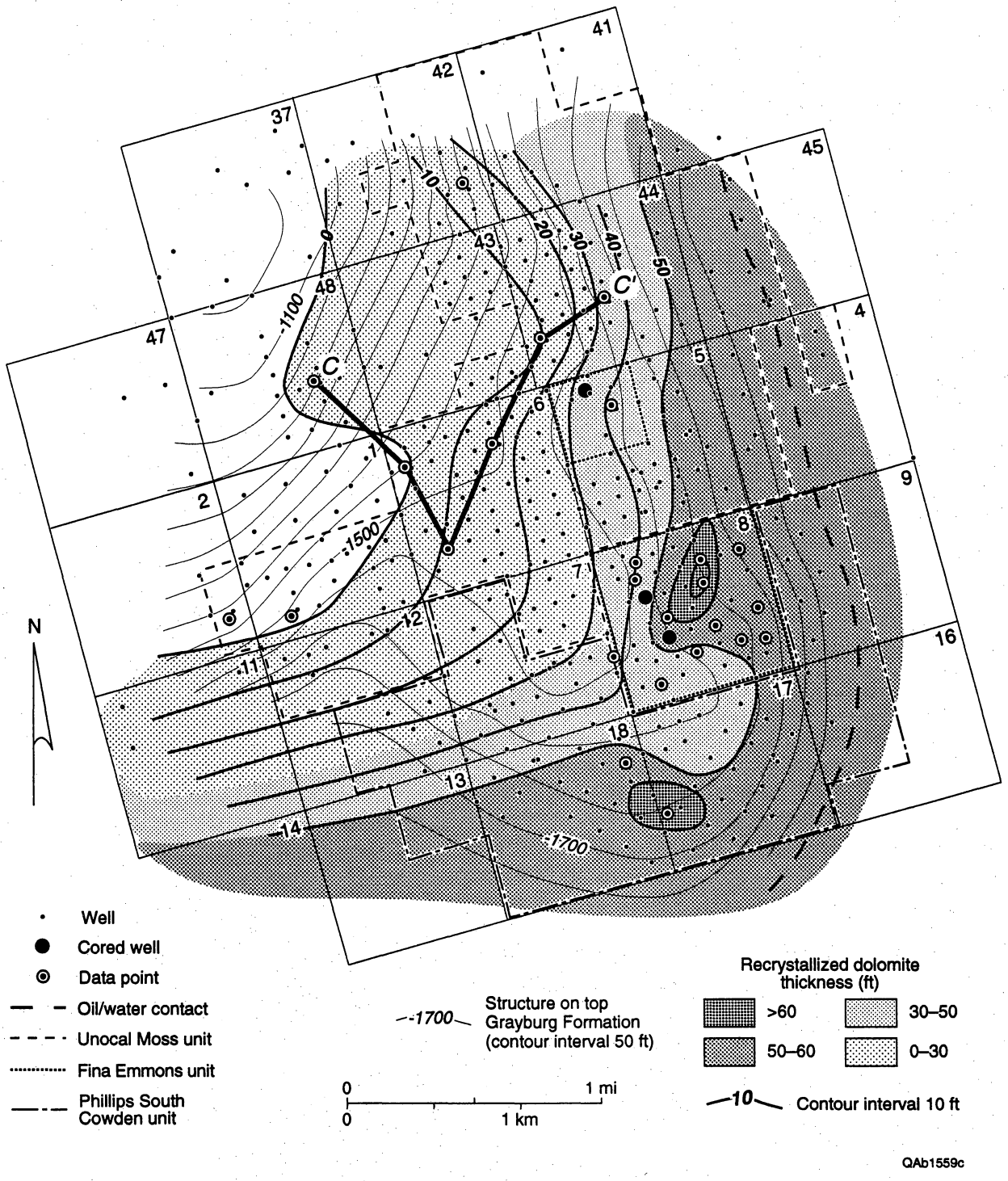

Figure 36. Map of South Cowden field showing the distribution of intervals of recrystallized dolomite. Note that they are most common on the outer margins of the field.

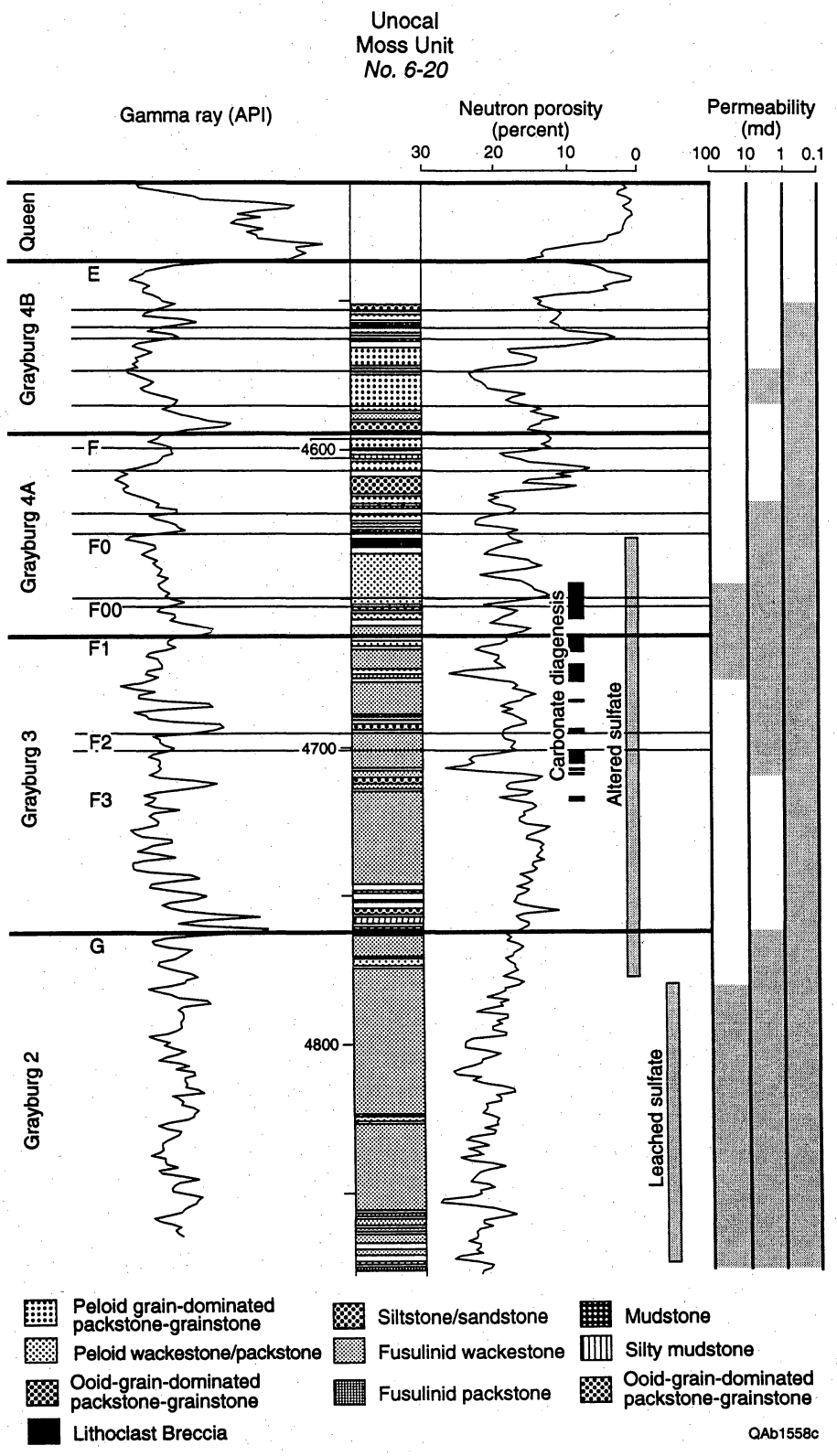

Figure 37. Distribution of zones of recrystallized dolomite and evidence of sulfate alteration and removal in the UNOCAL Moss Unit No. 6-20 well. Note that highest permeabilities in the well are developed in zones of recrystallized dolomite and massive sulfate removal. The latter is mostly below the field oil-water contact.

surrounding matrix for four cores in their South Cowden Unit (table 1). These analyses showed permeabilities of up to several orders of magnitude greater in recrystallized zones than in adjacent matrix. Porosities measured were as much as 5 times higher in recrystallized zones. Average values for all samples measured show porosity that was two times higher and permeability that was an order of magnitude higher (table 1).

Table 1. Comparison of porosity and permeability data from selected core plugs in South Cowden field (courtesy Phillips Petroleum Company).

Lithology	Samples	Average porosity (%)	Porosity range (%)	Average permeability (md)	Permeability range (md)
Unrecrystallized Dolomite matrix	34	10.0	1.8–26.1	22.55	0.00–442
Recrystallized Dolomite	34	21.2	9.1–35.7	211.37	0.28–5940

Petrographic analysis indicates that the causes of permeability and porosity increase in these recrystallized zones are twofold. First, larger dolomite crystal sizes and leached dolomite rhombs in these zones constitute a fabric that contains higher intercrystalline pore volume. Second, where anhydrite cement has been partially or completely removed from these zones, porosities are even further enhanced (fig. 38).

The cause and timing of dolomite leaching and recrystallization in the Grayburg highstand succession are not fully constrained. Previous studies have, however, recognized similar features in San Andres and Grayburg rocks. Bebout and others (1987) described features from the Grayburg in Dune field, which they referred to as the "vertically structured facies," that are virtually identical to recrystallized zones documented above. Like those in the South Cowden Grayburg succession, Dune field examples are developed in skeletal and peloidal wackestones and packstones. These rocks also display similar values for porosity and permeability.

Leary and Vogt (1990) and Major and others (1990) documented similar zones of altered dolomite in San Andres and Grayburg reservoir successions in several fields on the Central Basin Platform. Both of these studies showed that lighter colored zones of leached dolomite were depleted in $\delta^{18}O$ by as much as 3.5 ‰ PDB compared to darker colored unaltered zones. These

studies also demonstrated that altered zones contained higher porosities and Major and others (1990) documented an order of magnitude greater permeabilities in altered zones than in surrounding matrix.

Leary and Vogt (1990) suggested that altered zones may have been the product of selective early dolomitization of relatively more permeable zones in the original sediment, followed by later, more extensive, dolomitization of the surrounding matrix. Selective dolomitization of more permeable zones is consistent with the apparent association in the South Cowden Grayburg of these zones with vertically burrowed intervals. Burrowing may easily create more porous and permeable zones than surrounding unburrowed zones. Leary and Vogt (1990) also suggested that inclusion-free dolomite overgrowths common in altered zones may have formed during the later, more extensive dolomitization event. Major and others (1990) interpreted the isotope depletion observed in altered intervals to be the result of selective leaching of nonstoichiometric, Calcium-rich early dolomite, which forms rhomb cores. These interpretations are consistent with the diagenetic history postulated by Ruppel and Cander (1988a, b) for similar rocks.

None of the previous studies of these early dolomitization events considered the spatial relationships of recrystallized or altered fabrics in arriving at a causal mechanism for dolomite diagenesis. In South Cowden field, zones of altered or recrystallized dolomite have definite textural, stratigraphic, and geographic restrictions. These zones are developed almost exclusively in highstand, mud-dominated, peloidal high-frequency cycles in the eastern part of the field, and many appear to be associated with vertical burrows. Their apparent association with burrows suggests that burrows acted as higher permeability conduit through which diagenetic fluids preferentially passed. The concentration of these recrystallized zones below the F marker (fig. 35), a possible sequence boundary that separates the formally defined HFS 4 into upper and lower parts (fig. 14), raises the possibility that their development may be related to exposure at this surface. It may be that during sea-level fall, burrowed zones in Grayburg underwent preferential early diagenesis and dolomitization as high volumes of water were pumped through these conduits. The petrographic history of these and similar zones described from other San

Andres and Grayburg reservoirs, however, indicates that they may have remained open as fluid pathways until at least Queen time, when appropriate conditions for large volumes of brine generation and reflux were first conducive to large-scale dolomitization at the scale necessary to dolomitize the remaining Grayburg succession (see discussion above; Ruppel and Cander (1988a, b). Accordingly, the timing of the initial stabilization of these zones cannot be precisely determined; it may have also postdated Grayburg deposition.

The cause of the variations in spatial distribution of zones of recrystallized dolomite is unclear. Thickness patterns mimic the trend of the predominant paleotopography during Grayburg HFS 1 through HFS 3. By HFS 4 time and later, however, relief on this part of the Grayburg platform appears to have been minimal. The apparent increase in the abundance of these zones toward areas of previously deeper water may reflect more hospitable conditions for burrowing activity farther out on the platform or may instead indicate more efficient pumping of diagenetic fluids through existing burrows in this area. It is not clear from current data whether one or both of these mechanisms were active.

Alteration and Leaching of Anhydrite

Anhydrite is ubiquitous in both high-porosity and low-porosity Permian reservoir successions. Much of the Grayburg succession in South Cowden field is typical in that it contains common to abundant nodular and poikilotopic anhydrite and anhydrite cement. Similar to other middle Permian shallow-water carbonate reservoirs, nodular anhydrite is most common in subtidal, mud-dominated rocks, such as peloidal and fusulinid wackestones and packstones. Poikilotopic and void-filling anhydrite are common in all facies.

Along the eastern and southern margin of the field, however, is evidence of (1) alteration of anhydrite to gypsum or bassanite and (2) partial to complete removal of all sulfate (figs. 39 and 40). Altered anhydrite is characterized in megascopic samples by nodules that are entirely or partly composed of white, chalky sulfate. In thin section these zones are characterized by low interference colors and microcrystalline pores. Although these altered zones do not always

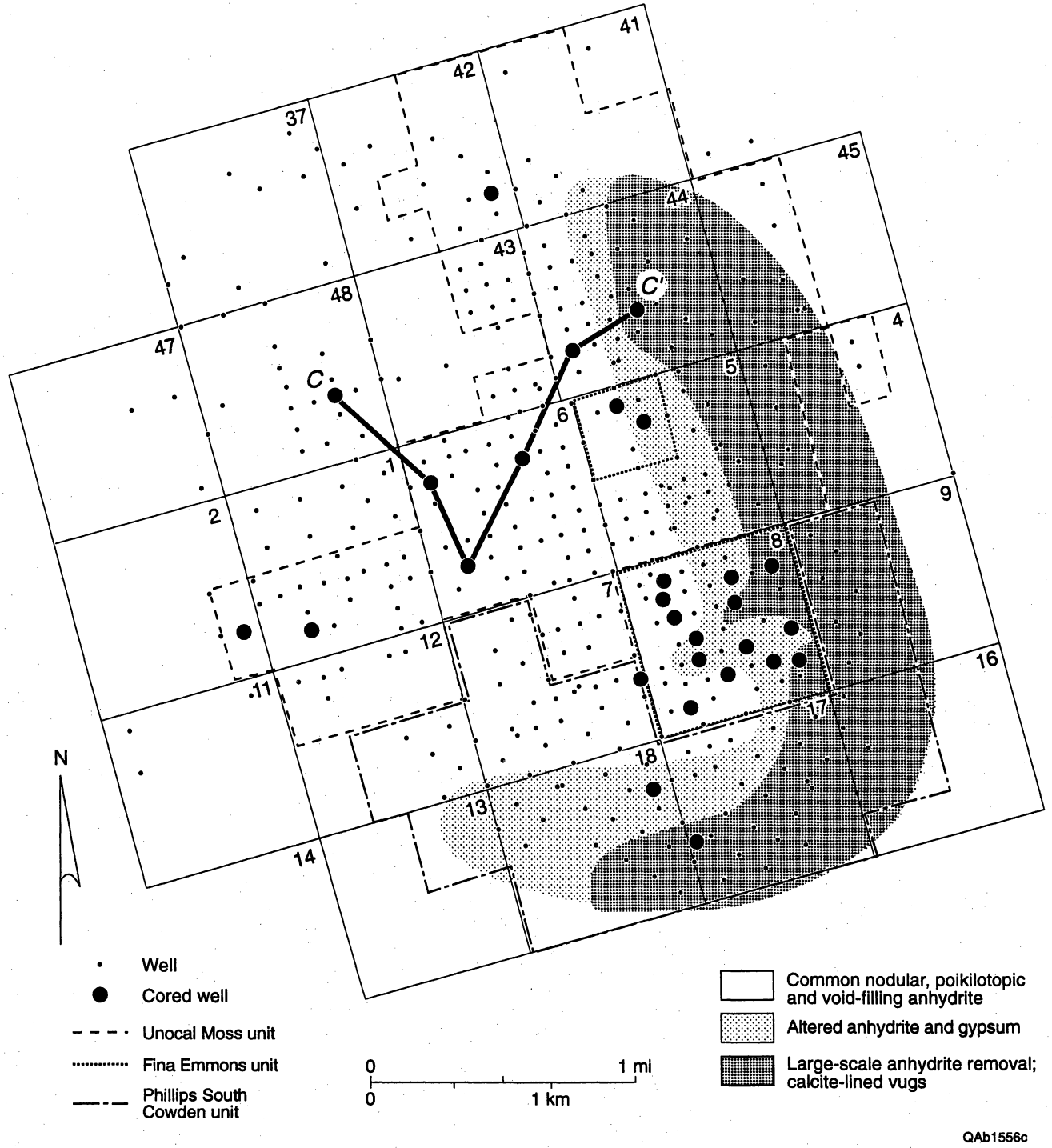

Figure 39. Map of the distribution of altered sulfate and intervals of complete sulfate removal in the South Cowden field.

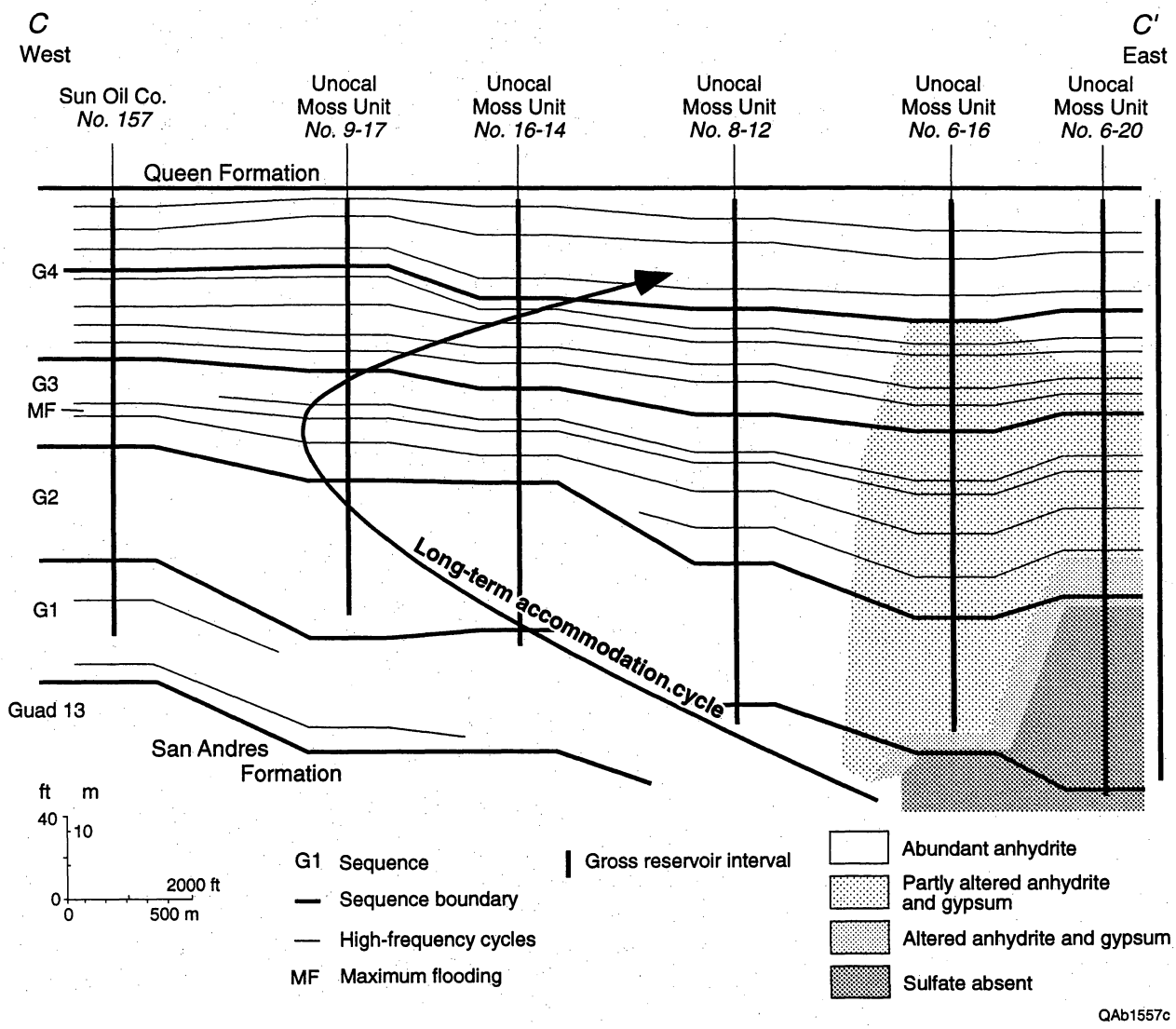

Figure 40. Dip cross section (C–C′) through the Moss Unit showing the distribution of altered sulfate and intervals of complete sulfate removal.

produce characteristic x-ray diffraction patterns of gypsum or bassanite, their style of alteration suggests that they are partially rehydrated anhydrite. Bebout and others (1987) reached similar conclusions on the basis of their examination of sulfate textures in the Grayburg Formation of Dune field. Intervals that contain evidence of altered anhydrite also typically contain zones of normal, apparently unaltered anhydrite.

Intervals in which sulfate has been completely removed are characterized by open pores of all sizes, including fusulinid molds, fractures, intercrystalline pores, and nodules. The latter are especially definitive evidence of sulfate removal, because no other origins for large spherical vugs in Permian shallow-water carbonate rocks are known. These nodules, molds, or vugs are commonly lined with calcite cement.

For the most part, intervals of total sulfate removal are restricted to depths below the nominal field oil/water contact (–1850 ft [–564 m]). In the UNOCAL No. 6-20 well in the eastern part of the field, for example, the top of this zone of sulfate removal is nearly exactly at this depth (fig. 40). Similar relationships are observed in some cored wells (No. 7-10, No. 8-19 in the South Cowden Unit) in the south part of the field. In the Fina Emmons Unit No. 135 cored well, however, the interval of near-complete sulfate removal extends almost 100 ft (30 m) higher in the section than elsewhere (fig. 41).

Patterns of vertical and lateral distribution demonstrate that alteration and removal of sulfate in the South Cowden field are related to structural position in the field (figs. 39 and 41). Because of this, sulfate diagenesis crosscuts facies and stratigraphy and is restricted to downdip parts of the field. The timing of this diagenesis cannot be precisely determined. Textural relationships indicate that it clearly postdates all dolomitization episodes and appears to have predated oil migration, however. Bebout and others (1987) postulated a prehydrocarbon migration meteoric flushing of the Dune reservoir on the basis of similar textural relationships. Calcite cements lining vugs of leached anhydrite nodules were probably precipitated during or slightly before oil migration. Similar calcites were shown by Leary and Vogt (1990) to have extremely depleted $\delta^{13}C$ values typical of calcites produced as a byproduct of sulfate reduction and bacterial

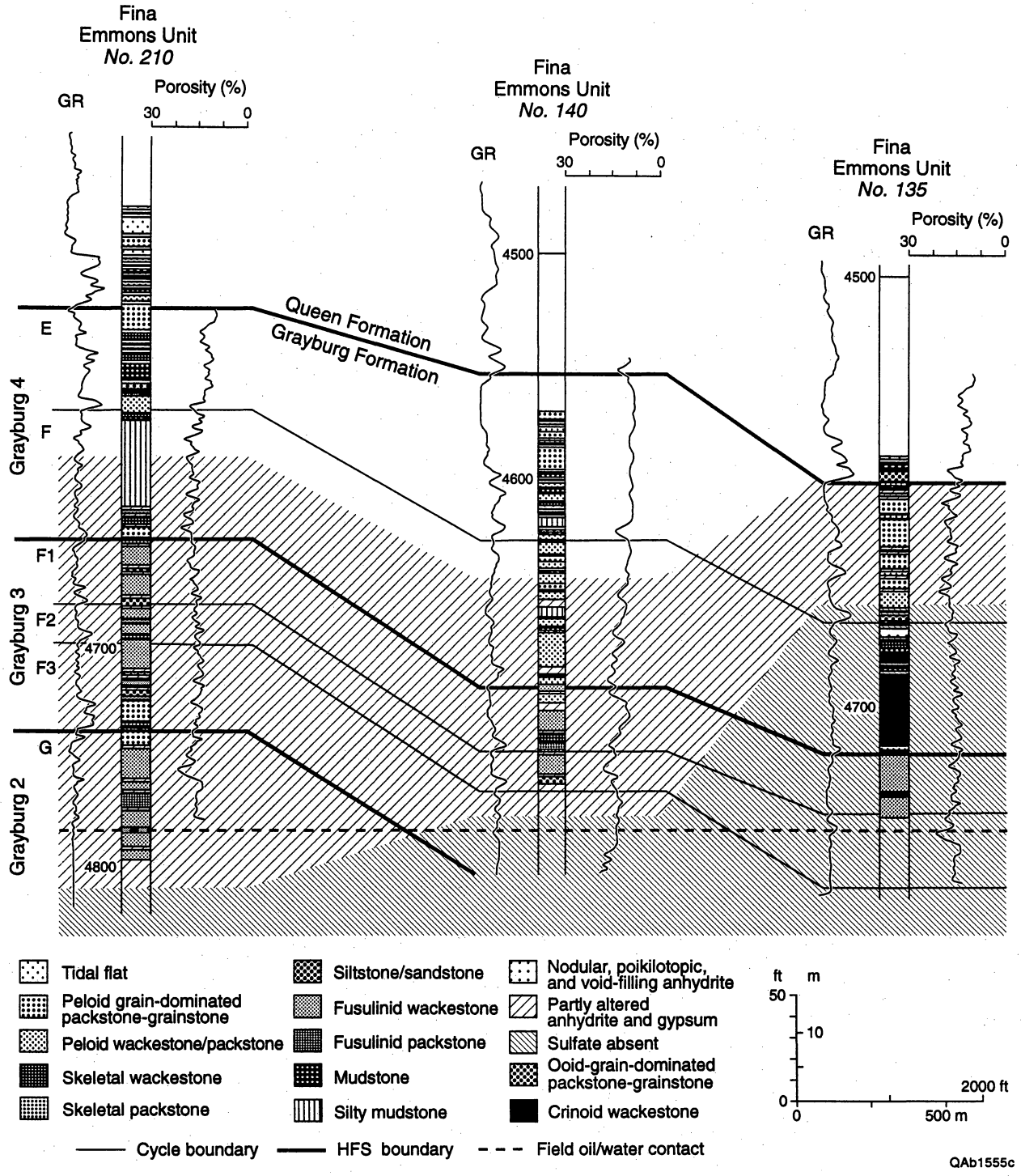

Figure 41. West-east cross section through part of the Emmons Unit showing the distribution of altered sulfate and intervals of complete sulfate removal. Note that in Fina Emmons Unit No. 135, the interval of complete sulfate removal extends about 100 ft (30 m) higher than in other cored wells.

oxidation of crude oil in the presence of meteoric fluids. Although the timing of oil migration has not been definitively established in the Permian Basin, preliminary data by Horak (1985) suggest migration began during the Mesozoic. The restriction of sulfate removal and diagenesis to downdip, basin-marginal positions in the field suggests that fluids responsible for leaching and sulfate removal may have been derived from the basin during a pre-oil migration phase of basin fluid expulsion.

Work by Lucia (in progress) demonstrates that sulfate content varies greatly in very short distances along the margins of the field. This work, which relates permeability to sulfate content and production volumes suggests that the process of sulfate removal left an extremely irregular plumbing system.

Where sulfate has been completely removed, both porosity and permeability are high (fig. 37). Porosities in these zones, which with few exceptions are restricted to below the oil/water contact, can range above 20 percent, whereas permeabilities commonly exceed 20 md and can range as high as several hundred millidarcys. Porosity and permeability in most areas of the reservoir where lesser amounts of sulfate diagenesis have occurred, can be equally high. Highest permeabilities in these intervals are observed where sulfate alteration or partial removal has affected zones of recrystallized dolomite (fig. 37). Permeabilities in these intervals match the highest in the field. Elsewhere in the field, porosities and permeabilities reflect a combination of the effects of sulfate diagenesis and original depositional textures.

EFFECTS OF STRATAL ARCHITECTURE VERSUS DIAGENESIS ON RESERVOIR DEVELOPMENT

The multihierarchical cyclicity dominant during Grayburg deposition exerted strong controls on the architectural style now characteristic of South Cowden and other Grayburg reservoirs in the Permian Basin. As a consequence, Grayburg reservoir successions contain distinctly different facies tracts and rock types whose distribution and character are a function of these controls. These original depositional textures constitute a basic control on the resultant rock

fabric and the petrophysics and flow unit characteristics of the reservoir. In South Cowden reservoir, however, these basic depositional controls are substantially overprinted by later diagenesis.

Gross porosity trends in South Cowden reflect primarily the diagenetic controls on reservoir development. Porosity × thickness maps for the bulk of the reservoir interval (HFS 3 and HFS 4) show maximum porosity trends coincident with areas of maximum effect of both dolomite and sulfate diagenetic events (compare fig. 30 with figs. 36 and 39). A similar trend is apparent for the HFS 3 sequence alone (fig. 31). Rocks in this sequence, however, have not been significantly affected by dolomite recrystallization but have been measurably influenced by sulfate diagenesis and removal. As mentioned above, more detailed work in progress (F. J. Lucia, personal communication, 1995) demonstrates small-scale variations in the effects of sulfate diagenesis and removal that play a major role in oil production success in the field.

Rocks in HFS 4 (lower part) have been most affected by dolomite recrystallization and much less so by sulfate alteration. Porosity development in these rocks (fig. 32) is first a function of dolomite diagenesis, second of sulfate alteration, and third of original depositional fabric. Where both diagenetic events are superimposed, reservoir quality is maximized.

Rocks of the upper part of HFS 4 are only locally affected by sulfate alteration. Additionally, the effects of dolomite diagenesis in this part of the section are variable. Although the abundance of recrystallized dolomite generally increases across the field to the east, the upper part of HFS 4 becomes grain rich to the east in the areas of the upper Grayburg ramp crest (fig. 29). Accordingly, much less burrow related recrystallization, which is typically restricted to mud-dominated intervals, is observed. Because of the absence of sulfate alteration and relatively little dolomite recrystallization, only slight porosity increases are observed (fig. 33).

Overall, the relative control of stratal architecture and original deposition facies textures increase upsection and to the interior (western part) of the field. Porosity trends in the interior part of the field, where the effects of the two later diagenetic events are largely absent, is much more strongly controlled by the original textures.

CONCLUSIONS

The Permian Grayburg Formation contains characteristic cycle stratigraphic elements that can serve as a fundamental basis for defining reservoir architecture. In South Cowden field, four high-frequency sequences are recognized as part of one longer term accommodation cycle. Sequence-scale elements document a depositional response to basic changes in accommodation, principally the result of relative rise and fall of sea level. Accordingly, these elements can be used for basinwide correlation of depositional sequences in Grayburg shallow-water platform successions in outcrop and the subsurface.

High-frequency cyclicity is well developed in much of the Grayburg succession and constitutes the basis for defining a high-resolution reservoir framework. In the South Cowden reservoir, high-frequency cycles are best developed in highstand, low-accommodation near ramp crest successions. Outer ramp cyclicity is definable where siliciclastics, accessed from the inner platform, have been reworked into cycle bases during maximum flooding but are less well developed in basal Grayburg transgressive sequences.

Despite the heterogeneity imparted by original variations in depositional textures in the Grayburg, mapping of porosity and permeability trends at South Cowden reveal that reservoir quality is strongly influenced by diagenesis. Two styles and periods of diagenesis are important. Relatively early recrystallization of dolomite was restricted to vertically borrowed zones in mud-dominated packstones and wackestones of cyclic highstand leeward ramp crest successions in HFS 3 and HFS 4. Later alteration and removal of anhydrite affected the outer, structurally low parts of the field. Highest porosity and permeability is developed where these events overlap, on the eastern and southern margins of the field. In these areas, original depositional texture exerts very little control on reservoir quality. The impact of depositional texture increases westward in the field as the overprint of these two diagenetic events lessens.

The cycle stratigraphic framework developed for the Grayburg at South Cowden field not only serves as a framework for high-resolution modeling and simulation of reservoir

performance but facilitates correlation, comparison, and modeling of other Grayburg successions in the Permian Basin.

Recognition of the extent and style of diagenetic overprint of original depositional facies demonstrates the importance of an integrated examination of depositional and diagenetic controls on reservoir development. Despite the significant development of diagenetically induced rock fabrics in the Grayburg Formation at South Cowden, effective modeling and simulation directed toward improving oil recovery efficiency in any Grayburg reservoir succession must start with the construction of a detailed, cycle stratigraphic-based reservoir framework.

REFERENCES

Babcock, J. A., 1977, Calcareous algae, organic boundstones, and the genesis of upper Capitan Limestone (Permian Guadalupian) Guadalupe Mountains, West Texas and New Mexico, *in* Hileman, M. E., and Mazzullo, S. J. eds., Upper Guadalupian facies, Permian reef complex, Guadalupe Mountains, New Mexico and West Texas: Permian Basin Section SEPM Publication 77-16, p. 3–44.

Barnaby, R. J., and Ward, W. B., 1994, Sequence stratigraphic framework, high-frequency cyclicity and 3-dimensional heterogeneity: Grayburg Formation, Brokeoff Mountains, New Mexico, *in* Pause, P. H., and Candelaria, M. P., eds., Carbonate facies and sequence stratigraphy: Practical applications of carbonate models: PBS-SEPM Publication 95-36, p. 37–50.

Bebout, D. G., Lucia, F. J., Hocott, C. R., Fogg, G. E., and Vander Stoep, G. W., 1987, Characterization of the Grayburg reservoir, University Lands Dune field, Crane County, Texas: The University of Texas at Austin, Bureau of Economic Geology Report of Investigations No. 168, 98 p.

Fischer, A. G., and Sarntheim, M., 1988, Airborne silts and dune-derived sands in the Permian of the Delaware Basin: Journal of Sedimentary Petrology, v. 58, p. 637–643.

Galloway, W. E., Ewing, T. E., Garrett, C. M., Jr., Tyler, Noel, and Bebout, D. G., 1983, Atlas of major Texas oil reservoirs: The University of Texas at Austin, Bureau of Economic Geology Special Publication, 139 p.

Handford, C. R., 1981, Sedimentology and genetic stratigraphy of Dean and Spraberry Formations (Permian) Midland Basin, Texas: American Association of Petroleum Geologists Bulletin, v. 65, no. 9, p. 1602–1616.

Harris, M. T., 1988, Sedimentology of the Cutoff Formation (Permian), Western Guadalupe Mountains, West Texas, *in* Reid, S. T., Bass, R. O., and Welch, P., eds., Guadalupe Mountains revisited—Texas and New Mexico: West Texas Geological Society Publication 88-84, p. 133–140.

Horak, R. L., 1985, Tectonic and hydrocarbon maturation in the Permian Basin: Oil and Gas Journal, v. 83, no. 21, p. 124–129.

Kerans, Charles, and Fitchen, W. M., 1995, Sequence hierarchy and facies architecture of a carbonate-ramp system: San Andres Formation of Algerita Escarpment and Western Guadalupe Mountains, West Texas and New Mexico: The University of Texas at Austin, Bureau of Economic Geology Report of Investigations No. 235, 86 p.

Kerans, Charles, and Fowler, David, 1995, Role of high-frequency cycles in analysis of ancient facies: an example from shelf-crest teepee-pisolite facies of the Guadalupian section, Guadalupe Mountains and subsurface of the Central Basin Platform, West Texas (abs.): American Association of Petroleum Geologists Official Program, 1995 Annual Convention, p. 49A.

Kerans, Charles, and Nance, H. S., 1991, High-frequency cyclicity and regional depositional patterns of the Grayburg Formation, Guadalupe Mountains, New Mexico, *in* Meader-Roberts, S., Candelaria, M. P., and Moore, G. E., eds., Sequence stratigraphy, facies and reservoir geometries of the San Andres, Grayburg and Queen Formations, Guadalupe Mountains, New Mexico and Texas: Permian Basin Section, Society of Economic Paleontologists and Mineralogists Publication 91-32, p. 53–96.

Kerans, Charles, and Ruppel, S. C., 1994, San Andres sequence framework, Guadalupe Mountains: Implications for San Andres type section and subsurface reservoirs, *in* Garber, R. A., and Keller, D. R., eds., Field guide to the Paleozoic section of the San Andres Mountains: Permian Basin Section, SEPM Publication 94-35, p. 105–116.

Kerans, Charles, Lucia, F. J., Senger, R. K., Fogg, G. E., Nance, H. S., and Hovorka, S. D., 1993, Characterization of facies and permeability patterns in carbonate reservoirs based on outcrop analogs: Fossil Energy, U.S. Department of Energy, final contract report, DOE/BC/14470-10, 160 p.

Kerans, Charles, Lucia, F. J., and Senger, R. K., 1994, Integrated characterization of carbonate ramp reservoirs using Permian San Andres Formation outcrop analogs: American Association of Petroleum Geologists, v. 78, no. 2, p. 181–216.

King, P. B., 1948, Geology of the southern Guadalupe Mountains: U.S. Geological Survey Professional Paper 215, 183 p.

Leary, D. A., and Vogt, J. N., 1990, Diagenesis of the San Andres Formation (Guadalupian) reservoirs, University Lands, Central Basin Platform, *in* Bebout, D. G., and Harris, P. M., (eds.), Geologic and engineering approaches in evaluation of San Andres/Grayburg hydrocarbon reservoirs—Permian Basin: The University of Texas at Austin, Bureau of Economic Geology Publication, p. 21–28.

Longacre, S. A., 1990, The Grayburg reservoir, North McElroy Unit, Crane County, Texas, *in* Bebout, D. G., and Harris, P.M. (eds.), Geologic and engineering approaches in evaluation of San Andres/Grayburg hydrocarbon reservoirs—Permian Basin: The University of Texas at Austin, Bureau of Economic Geology Publication, p. 239–273.

Lucia, F. J., Wang, F., and Kerans, Charles, 1995, Rock-fabric approach to reservoir characterization: Seminole San Andres Unit, Gaines County, Texas: Report of the RCRL, annual meeting, Carlsbad, New Mexico, October 18, 1995, 42 p.

Major, R. P., Bebout, D. G., and Lucia, F. J., 1988, Depositional facies and porosity distribution, Permian (Guadalupian) San Andres and Grayburg Formations, P.J.W.D.M. Field Complex, Central Basin Platform, West Texas, *in* Giant oil and gas fields—a core workshop: SEPM Core Workshop No. 12, p. 615–648.

Major, R. P., Vander Stoep, G. W., and Holtz, M. H., 1990, Delineation of unrecovered mobile oil in a mature dolomite reservoir: East Penwell San Andres Unit, University Lands, West Texas: The University of Texas at Austin, Bureau of Economic Geology Report of Investigations No. 194, 52 p.

Pray, L. C., 1988, The Western Escarpment of the Guadalupe Mountains, Texas and Day Two of the Field Seminar, *in* Reid, S. T., Bass, R. O., and Welch, P., eds., Guadalupe Mountains revisited—Texas and New Mexico: West Texas Geological Society Publication 88-84, p. 23–31.

Rossen, C., and Sarg, J. F., 1988, Sedimentology and regional correlation of a basinally restricted deep-water siliciclastic wedge: Brushy Canyon Formation–Cherry Canyon Tongue (Lower Guadalupian), Delaware Basin, *in* Reid, S. T., Bass, R. O., and Welch, P., eds., Guadalupe Mountains revisited—Texas and New Mexico: West Texas Geological Society Publication 88-84, p. 127–132.

Ruppel, S. C., 1992, Styles of deposition and diagenesis in Leonardian carbonate reservoirs in West Texas: implications for improved reservoir characterization: Society of Petroleum Engineers Annual Exhibition and Technical Conference, 24691, p. 313–320.

Ruppel, S. C., and Cander, H. S., 1988a, Dolomitization of shallow-water platform carbonates by seawater and seawater-derived brines: San Andres Formation (Guadalupian), West Texas, *in* Sedimentology and geochemistry of dolostones: Society of Economic Paleontologists and Mineralogists, Special Publication No. 43, p. 245–262.

_____ 1988b, Effects of facies and diagenesis on reservoir heterogeneity: Emma San Andres field, West Texas: The University of Texas at Austin, Bureau of Economic Geology Report of Investigations No. 178, 67 p.

Ruppel, S. C., Kerans, Charles, Major, R. P., and Holtz, M. H., 1995, Controls on reservoir heterogeneity in Permian Basin shallow-water-platform carbonate reservoirs, Permian Basin: implications for secondary recovery: The University of Texas at Austin, Bureau of Economic Geology Geological Circular 95-2, 30 p.

Sonnenfeld, M. D., 1991, High-frequency cyclicity within shelf-margin and slope strata of the upper San Andres sequence, Last Chance Canyon, *in* Meader-Roberts, Sally, Candelaria, M. P., and Moore, G. E., eds., Sequence stratigraphy, facies and reservoir geometries of the San Andres, Grayburg, and Queen Formations, Guadalupe Mountains, New Mexico and Texas: Permian Basin Section, Society of Economic Paleontologists and Mineralogists Publication 91-32, p. 11–51.

Tyler, Noel, Galloway, W. E., Garrett, C. M., Jr., and Ewing, T. E., 1984, Oil accumulation, production characteristics, and targets for additional recovery in major oil reservoirs of Texas: The University of Texas at Austin, Bureau of Economic Geology Geological Circular 84-2, 31 p.

Tyler, Noel, and Banta, N. J., 1989, Oil and gas resources remaining in the Permian Basin: targets for additional hydrocarbon recovery: The University of Texas at Austin, Bureau of Economic Geology Geological Circular 89-4, 20 p.

Tyler, Noel, Major, R. P., Bebout, D. G., Kerans, Charles, Lucia, F. J., Ruppel, S. C., and Holtz, M. H., 1992, Styles of heterogeneity in dolomitized platform carbonate reservoirs: examples from the Central Basin Platform of the Permian Basin, southwestern U.S.A.: Journal of Petroleum Science and Engineering, v. 6, p. 301–339.

Young, Addison, and Vaughn, J. C., 1957, Addis–Johnson–Foster–South Cowden field, in Herald, F. A., ed., Occurrence of oil and gas in West Texas: Austin, The University of Texas Publication No. 5716, p. 17–22.